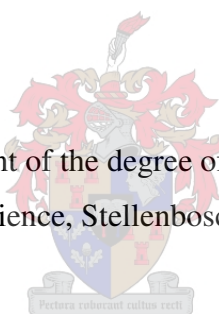# Preparation and Coordination Chemistry of Bis-Pyridyl Diamide Ligands

by

Eustina Batisai

Thesis presented in partial fulfilment of the degree of Master of Science in Chemistry at Faculty of Science, Stellenbosch University

Supervisor

Professor L. J. Barbour

Co-supervisor

Dr. T. le Roex

March 2010

Chapter 4

Coordination Chemistry of Bis-Pyridyl Diamide Ligands

4.1   Introduction

One of the main strategies employed in crystal engineering is the use of coordination bonding.[1] By careful choice of the metal ion,[2] the nature of the ligand[3] and given the high directionality of the coordination bond[4,5], molecular networks with interesting topologies and structural features such as gas storage,[6] and chemical sensing[7] have been constructed. A versatile strategy that has been recently recognized is the combination of the coordination bond and the hydrogen bond and other weaker interactions such as π-π interactions in the construction of molecular networks.[8] This strategy has been employed in this work by utilizing the coordination bonding ability of the bis-pyridyl moiety and the hydrogen bonding ability of the amide functional group.[5,9]

A total of seventeen novel crystal structures obtained from the reaction conditions outlined in section 2.2 are described here. The crystallographic data and details of the structure solution and refinement procedures for compounds **1**-**17** are given at the end of the chapter (pages 94-97). Crystal structures of coordination complexes of **DIP** and **TER** were not obtained as part of this study.

4.2   Results and discussion: Crystal structure determinations from SCD analysis.

4.2.1   Crystal structures obtained with FUM

4.2.1.1 {[Cu(**FUM**)(H$_2$O)$_3$]·(SO$_4$)·(H$_2$O)$_2$}$_n$ **1**
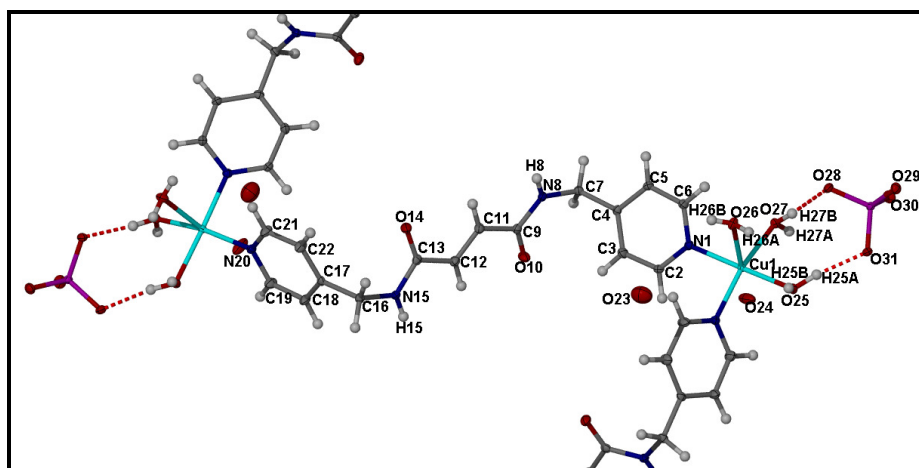

Figure 4.1. The molecular structure of **1** showing crystallographic labelling scheme and 50% probability ellipsoids for non-hydrogen atoms. Only the asymmetric unit is labelled.

Crystals suitable for SCD analysis were grown by slow evaporation of a solution containing the ligand **FUM** and $CuSO_4$ in a M:L ratio of 4:1. The compound crystallizes in the monoclinic space group $P2_1/c$. The asymmetric unit (Figure 4.1) consists of one Cu(II) cation, one complete **FUM** molecule, one sulphate anion, two uncoordinated water molecules and three coordinated water molecules. The Cu(II) cation adopts a distorted trigonal bipyramidal geometry and the coordination geometric parameters are given in Table 4.1. The metal centres are linked by bridging **FUM** ligands to form 1-D zigzag chains running along [100]. Each 1-D chain interacts with its neighbours *via* sulphate anions and coordinated water molecules to form a 2-D network (Figure 4.2).
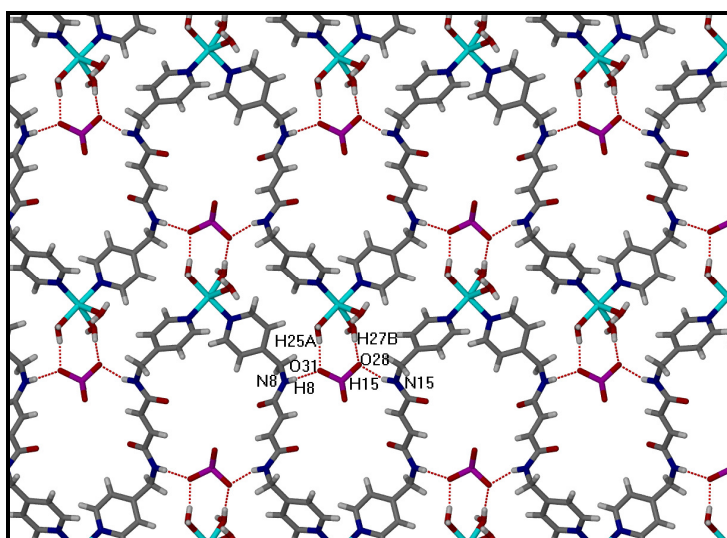

Figure 4.2. Capped stick representation of 2-D hydrogen bonded network of **1** formed as a result of interactions between the amide groups, the sulphate anions and coordinated water molecules. Only the atoms involved in hydrogen bonding are labelled.

Table 4. 1. Coordination geometric parameters (Å, °) for **1**

Distance	
Cu1 − O27	1.986(1)
Cu1 − N20^i	2.006(2)
Cu1 − N1	2.011(2)
Cu1 − O25	2.027(2)
Cu1 − O26	2.284(2)
Angle	
O27 − Cu1 − N20^i	168.7(7)
O27 − Cu1 − N1	91.7(7)
O27 − Cu1 − O25	89.7(7)
O27 − Cu1 − O26	86.4(6)
N20^i − Cu1 − N1	94.2(8)
N20^i − Cu1 − O25	85.3(8)
N20^i − Cu1 − O26	103.40(8)
N1 − Cu1 − O26	175.4(6)
N1 − Cu1 − O25	88.6(7)
O25 − Cu1 − O26	87.2(7)

Symmetry codes (i) *x, -y+3/2, z-1/2*

Two of the coordinated water molecules on one chain are hydrogen bonded to a sulphate anion (O25−H25A⋯O31 and O27−H27B⋯O28) which is in turn hydrogen bonded to two of the ligands in the consecutive chain *via* the amide NH group (N8−H8O⋯31[ii] and N15−H15O⋯28[iii]) (Figure 4.2).

Table 4.2. Hydrogen-bond geometry (Å, °) for **1**

X−H⋯A	X−H	X⋯A	D⋯A	∠(XHA)
N8−H8⋯O31[ii]	0.88	1.97	2.824(2)	164
N15−H15⋯O28[iii]	0.88	1.98	2.821(2)	160
O26−H26A⋯O29[vi]	0.96	1.96	2.758(2)	157
O27−H27B⋯O28	0.96	1.75	2.656(2)	171
O25−H25A⋯O31	0.96	1.78	2.682(2)	168
O27−H27A⋯O30[v]	0.96	1.82	2.728(2)	169
O25−H25B⋯O29[vi]	0.96	2.13	2.821(2)	156
O26−H26B⋯O14[vi]	0.96	2.06	2.721(2)	153

Symmetry codes: (ii) *x*, -*y*+1/2, *z*+1/2, (iii) *x*, *y*+1, *z*, (vi) -*x*+1,-*y*,-*z*, (v) -*x*+2, -*y*, -*z*, (vi) -*x*+1, *y*-1/2,-*z*+1/2
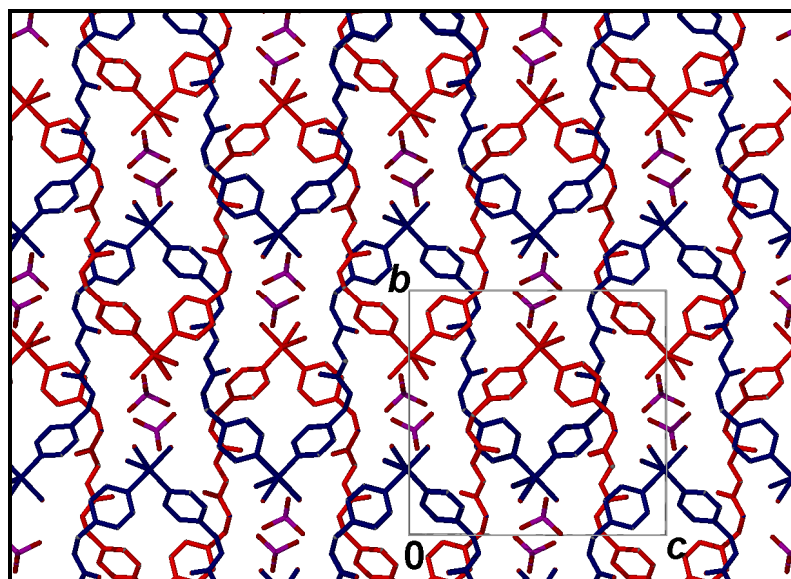

Figure 4.3. Packing diagram of **1**. Chains in alternate layers are shown in red and blue to distinguish them from each other, the sulphate anions are shown in CPK colours. The water molecules and hydrogen atoms have been omitted for clarity.

The 2-D networks stack in layers parallel to the *bc* plane, with alternate layers displaced by half a unit cell length along [010] and by half a unit cell length along [001]. The chains in the two adjacent layers are arranged in an ...ABABA… fashion such that chains in the first layer directly overlay the chains in the third layer (Figure 4.3). In addition to linking chains within a layer, the sulphate anions also link the layers *via* four further hydrogen bonds (O25−H25B⋯O29[vi], O26−H26A⋯O29[vi], O27−H27A⋯O30[v] and O25−H25A⋯O31) to

coordinated water molecules in adjacent layers (Figure 4.4). These hydrogen bonding interactions result in a 3-D network.
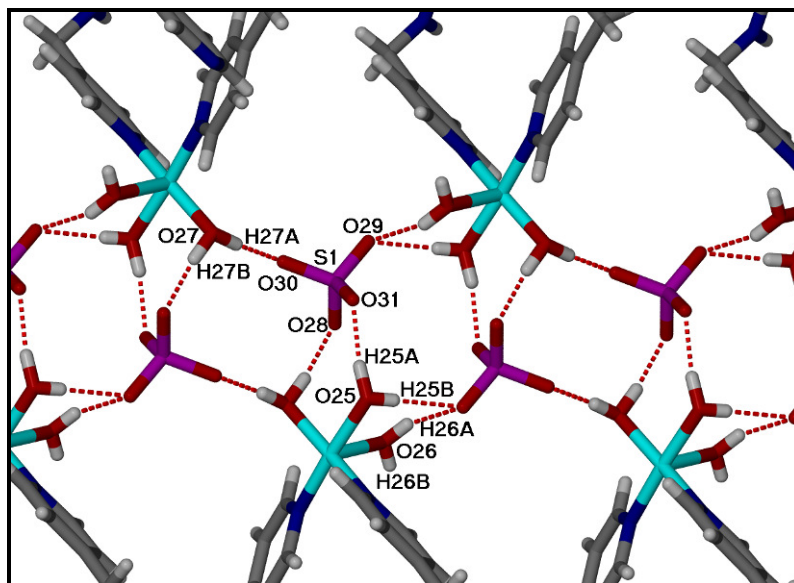

Figure 4.4. Expanded view of the hydrogen bonding interactions between layers in **1**, sulphate anions link the chains in alternate layers *via* hydrogen bonding to coordinated water molecules.

The adjacent layers are also connected by a hydrogen bond between the amide carbonyl group of a chain in one layer and the coordinated water molecule of a chain in the next layer (O26－H26B·····O14^{vi}). All hydrogen bonding details are given in Table 4.2.

4.2.1.2 {[Cu(FUM)(H₂O)₄]·(NO₃)₂·(H₂O)₂}ₙ 2
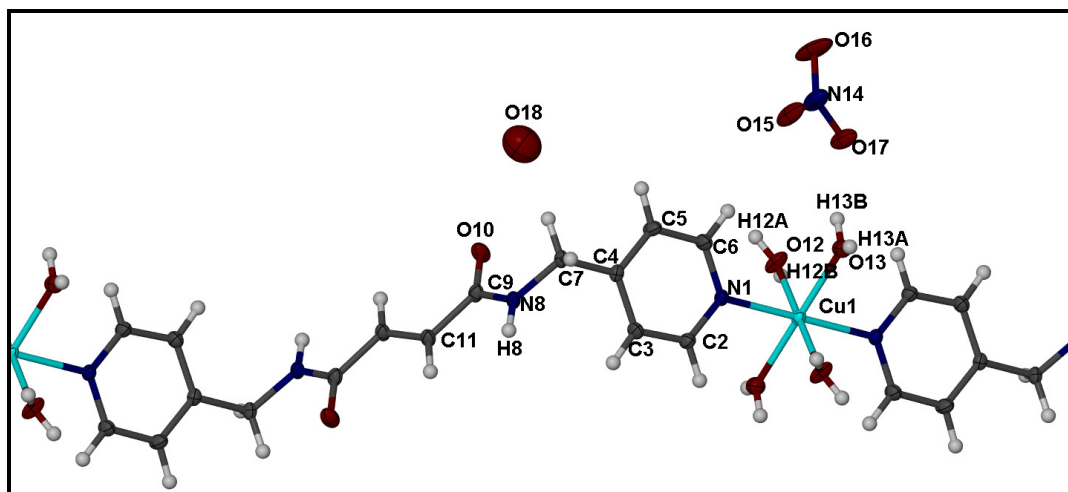

Figure 4.5. The molecular structure of **2** showing the crystallographic labelling scheme and 50% probability ellipsoids for non-hydrogen atoms. Only the asymmetric unit is labelled.

Crystals suitable for SCD analysis were grown by slow evaporation of an ethanolic solution of **FUM** and Cu(NO₃)₂ in a M:L ratio of 4:1. The asymmetric unit (Figure 4.5) consists of half a

FUM molecule, half a Cu(II) cation, one nitrate anion, two coordinated water molecules and an uncoordinated water molecule. The Cu(II) centre which is coordinated to two nitrogen atoms of two **FUM** ligands and four water molecules, adopts a distorted octahedral geometry (Table 4.3). The ligand links metal centres into continuous 1-D chains, running along [011].
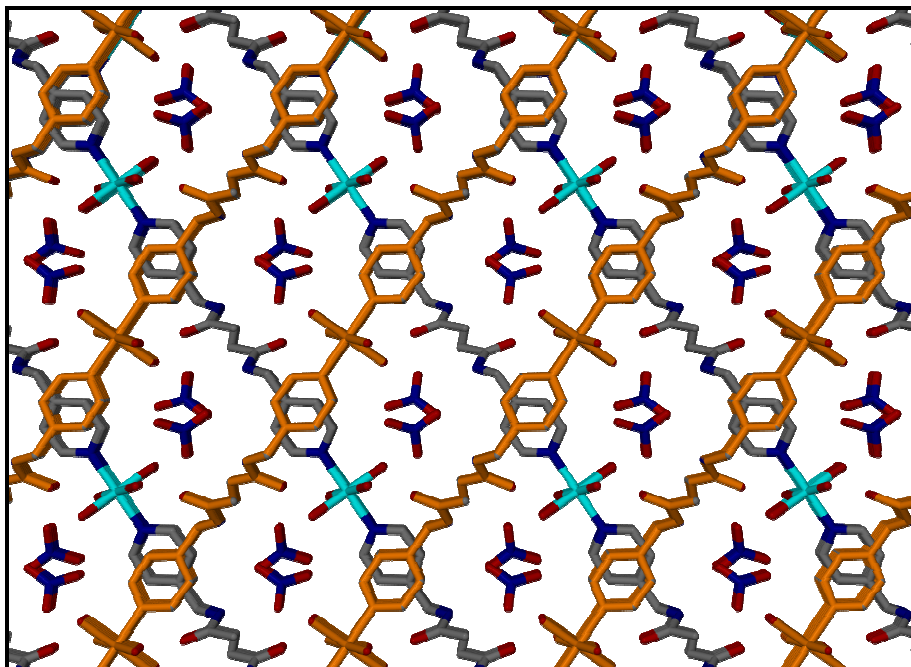

Figure 4.6. The packing diagram of **2** as viewed along [001]. Chains in adjacent layers are shown in CPK colours and in light brown.

The 1-D chains pack to form undulating layers parallel to [011], with chains in alternate layers running approximately perpendicular to each other (Figure 4.6). The layers pack in an …ABAB… fashion. The nitrate anions connect chains within the same layer into a 2-D network, by hydrogen bonding to the amide group of one chain (N8－H8⋯O15[ii]), as well as to a coordinated water molecule of the adjacent chain (O12－H12A⋯O16[v], Figure 4.7). The parallel 1-D chains in the same layer interact with those in the adjacent layer *via* four types of hydrogen bonds. Three of these occur *via* the nitrate counter ion (N8－H8⋯O15[ii], O13－H13B⋯O15 and O12－H12A⋯O16[v]), while the fourth hydrogen bond is a direct interaction between a coordinated water molecule of a chain in one layer and the carbonyl group of a chain in the adjacent layer (O12－H12B⋯O10[v]).

Table 4.3. Coordination geometric parameters (Å, º) for **2**

Distance		Angle	
Cu1 ─ O13	2.045(2)	O13 ─ Cu1 ─ O13^i	180.0(1)
Cu1 ─ O13^i	2.045(2)	O13 ─ Cu1 ─ O12	91.6(1)
Cu1 ─ O12	2.049(2)	O13 ─ Cu1 ─ O12^i	88.4(1)
Cu1 ─ O12^i	2.049(2)	O13 ─ Cu1 ─ N1	91.1(1)
Cu1 ─ N1	2.099(2)	O13 ─ Cu1 ─ N1^i	88.9(1)
Cu1 ─ N1^i	2.099(2)	O12^i ─ Cu1 ─ N1	92.3(1)
Angle		O12^i ─ Cu1 ─ N1^i	87.7(1)
O13^i ─ Cu1 ─ O12	88.4(1)	N1 ─ Cu1 ─ N1^i	180.0(2)
O13^i ─ Cu1 ─ O12^i	91.6(1)		
O13^i ─ Cu1 ─ N1	88.9(1)		
O13^i ─ Cu1 ─ N1^i	91.1(1)		
O12 ─ Cu1 ─ O12^i	180.0(2)		
O12 ─ Cu1 ─ N1	87.7(1)		
O12 ─ Cu1 ─ N1^i	92.3(1)		

Symmetry codes: (i) -*x*+1, -*y*, -*z*

There is one further hydrogen bond between the uncoordinated water molecule and one of the coordinated water molecules (O13 ─ H13A⸱⸱⸱⸱O18^{iii}, O13 ─ H13A⸱⸱⸱⸱O18^{vi}). The hydrogen bonding is shown in Figure 4.8 and details of all hydrogen bonds in the structure are given in Table 4.4
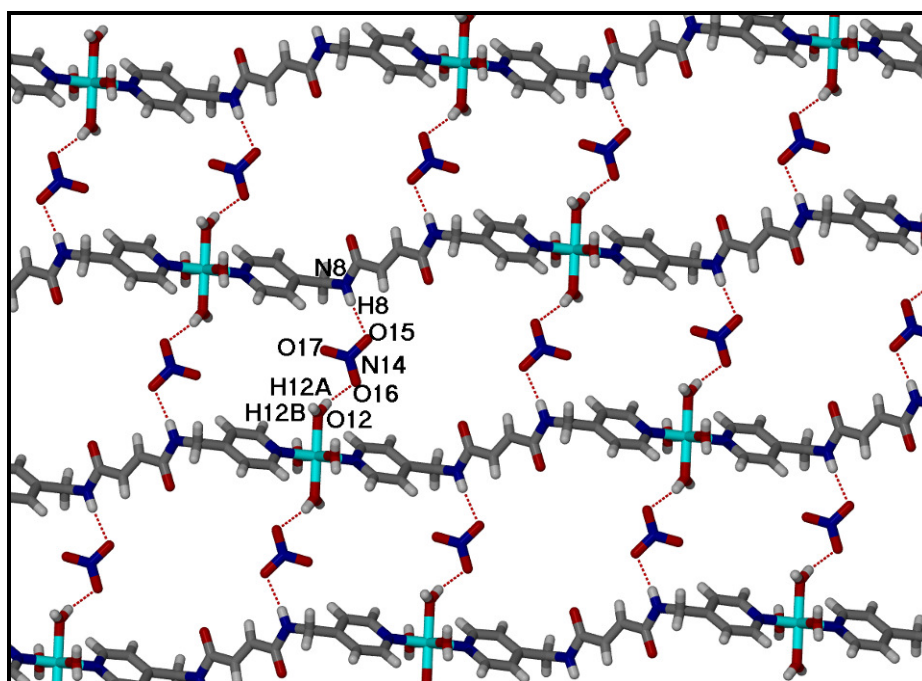

Figure 4.7. Hydrogen bonding interactions between chains in the same layer in **2**. The 1-D chains interact *via* the nitrate anion. Only the atoms involved in hydrogen bonding have been labelled.

Table 4.4. Hydrogen-bond geometry (Å, °) for **2**

X−H⋯A	X−H	H⋯A	X⋯A	∠(XHA)
N8−H8⋯O15^{ii}	0.88	2.08	2.870(3)	148
O13−H13B⋯O15	0.96	1.77	2.709(3)	166
O13−H13A⋯O18^{iii}	0.96	1.85	2.770(5)	160
O13−H13A⋯O18^{vi}	0.96	1.95	2.708(6)	135
O12−H12A⋯O16^{v}	0.96	1.82	2.738(3)	158
O12−H12B⋯O10^{vi}	0.96	1.80	2.713(4)	159

Symmetry codes: (ii) *x*-1, -*y*+1/2, *z*-1/2, (iii) x, -*y*+1/2, *z*+1/2, (vi) -*x*+1, *y*-1/2, -*z*+1/2, (v) -*x*+1, *y*-1/2, -*z*+1/2, (vi) -*x*+1, *y*-1/2, -*z*+1/2, (vii) *x*, -*y*+1/2, *z*+1/2
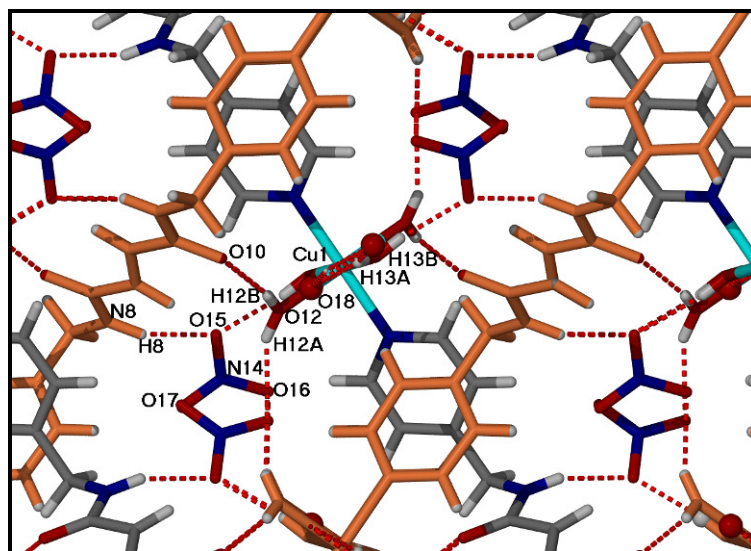

Figure 4.8. An expansion of hydrogen bonding interactions between chains in **2**. The chains are shown in light brown and in CPK colours. Only the atoms involved in hydrogen bonding have been labelled.

4.2.1.3 {[Ni(**FUM**)(H$_2$O)$_4$]·(H$_2$O)$_2$·Cl$_2$}$_n$ **3**

Crystals suitable SCD analysis were grown by slow evaporation of a solution of **FUM** and Ni(NO$_3$)$_2$ in an M:L ratio of 4:1 in ethanol. The complex crystallizes in the monoclinic space group *P*2$_1$/*c*. The asymmetric unit (Figure 4.9) consists of half a **FUM** molecule, half a Ni(II) cation, one chloride anion, one uncoordinated water molecule and two coordinated water molecules. The metal centre which is coordinated to two nitrogen atoms of two ligands and four water molecules, adopts a distorted octahedral geometry. The coordination geometric parameters are given in Table 4.5.
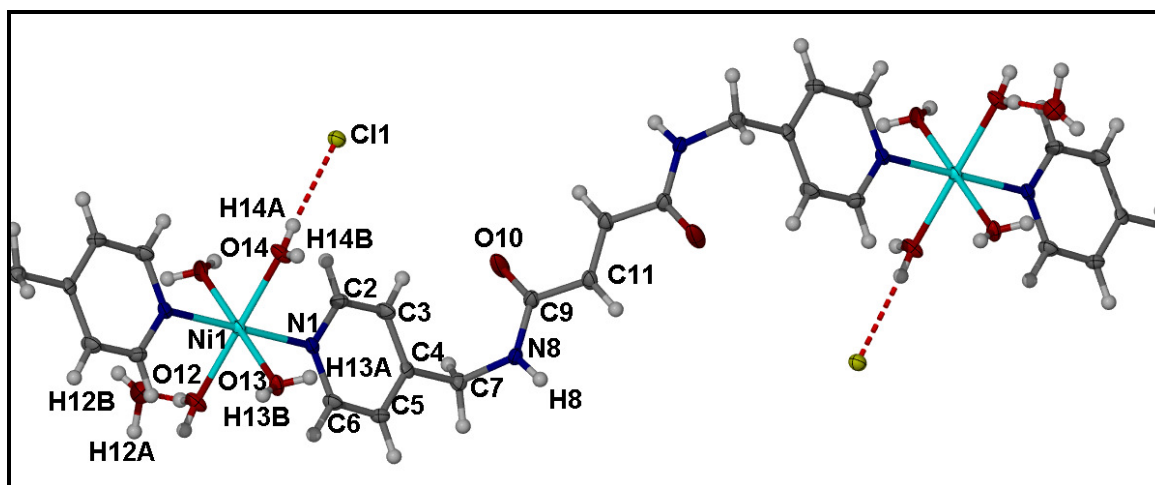
Figure 4.9. The molecular structure of **3** showing the crystallographic labelling scheme for the asymmetric unit and 50% probability ellipsoids for non-hydrogen atoms. Red dashed lines indicate hydrogen bonding,

Table 4.5. Coordination geometric parameters (Å, º) for **3**

Distance		Angle	
Ni1－O14^i	2.060(2)	O14^i－Ni1－O14	180.0(2)
Ni－O14	2.060(2)	O14^i－Ni1－O13	88.6(1)
Ni1－O13	2.078(2)	O14^i－Ni1－O13^i	91.4(1)
Ni1－O13^i	2.078(2)	O14^i－Ni1－N1^i	88.1(1)
Ni1－N1	2.077(2)	O14i－Ni1－N1	91.9(1)
Ni1－N1^i	2.077(2)	O13^i－Ni1－N1^i	91.41(1)
Angle		O13^i－Ni1－N1	88.6(1)
O14－Ni1－O13	91.4(1)	N1^i－Ni1－N1	180.0(1)
O14－Ni1－O13^i	88.6(1)		
O14－Ni1－NI	91.9(1)		
O14－Ni1－N1^i	88.1(1)		
O13－Ni1－O13^i	180.0(2)		
O13－Ni1－N1	88.6(1)		
O13－Ni1－N1^i	91.41(2)		

Symmetry codes: (i) *x*+1, -*y*, -*z*

The metal centres are linked by a single bridging ligand to form 1-D chains along [001]. The 1-D chains pack to form layers in the *ab* plane, with chains in alternate layers perpendicular to each other as shown in Figure 4.10. Consecutive chains within the same layer are held together by hydrogen bonding *via* the chloride anion which hydrogen bonds to one chain *via* the amide nitrogen atom (N8－H8⋯Cl1^{ii}) and to the following chain *via* a coordinated water molecule (O14－H14A⋯Cl^{iii}) (Figure 4.11). The layers are held together by four pairs of hydrogen bonds *via* the chloride anion, (O13－H13B⋯Cl1⋯H8－N8, O12－H12A⋯Cl1⋯H14A－O14, O14－H14A⋯Cl⋯H8－N8 and O14－H14A⋯Cl1⋯H13B－O13) as well as a hydrogen bond between a coordinated water molecule of a chain in one layer and an amide carbonyl group of a chain in the adjacent layer (O13－H13⋯O10^{iii}). There is one further hydrogen bond between the uncoordinated water

molecule and one of the coordinated water molecules (O14－H14B⋯O12). A perspective view of the hydrogen bond interaction between layers is shown in Figure 4.12 and all hydrogen bond details are given in Table 4.6.
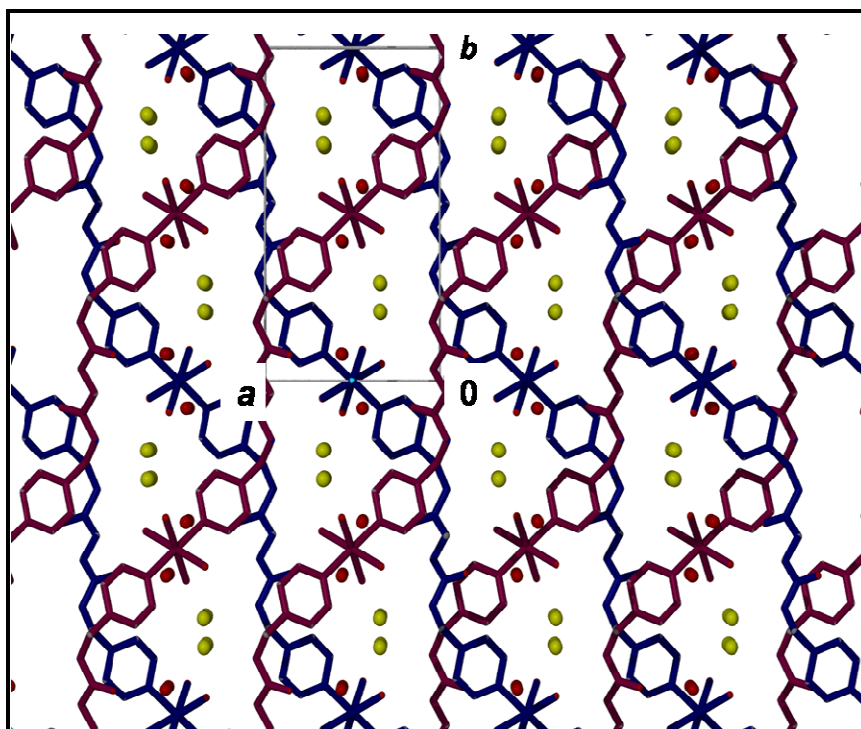

Figure 4.10. The packing diagram of **3** as viewed along [001]. Chains in different layers have been coloured in blue and maroon to distinguish them from one another. Hydrogen atoms have been omitted for clarity.
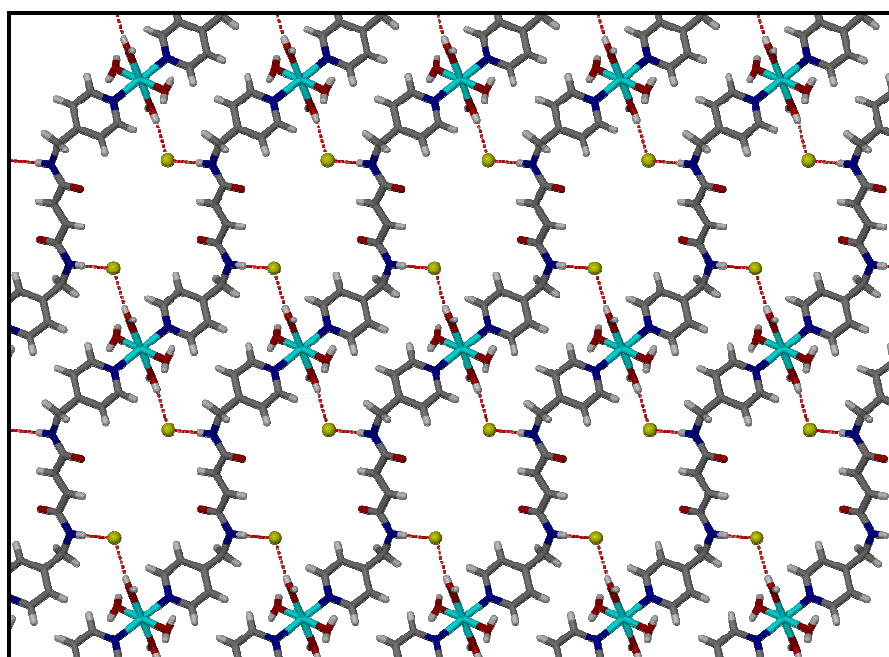

Figure 4.11. The 2-D network formed as a result of hydrogen bonding between 1-D chains and the chloride anion in **3**.
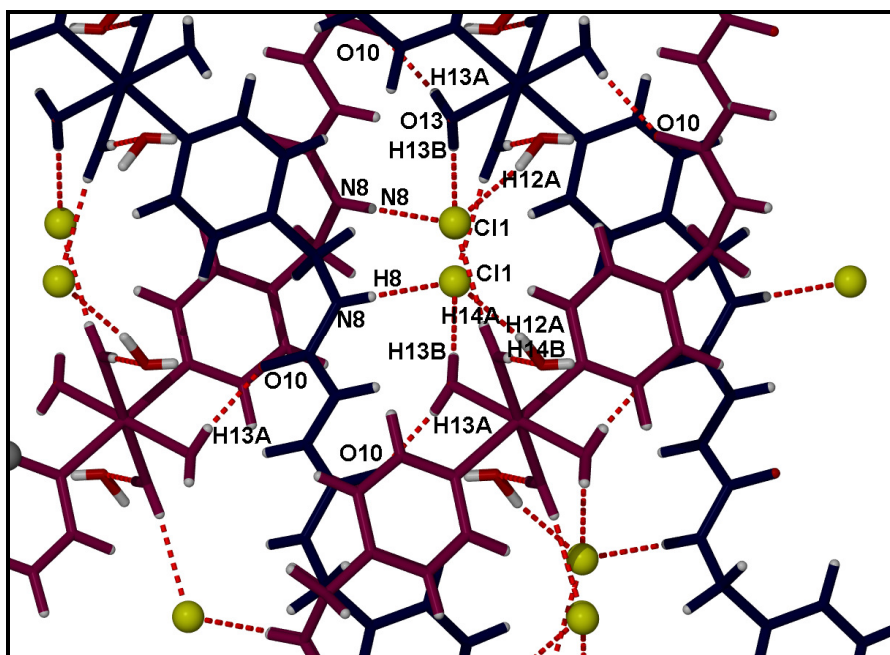
Figure 4.12. An expansion of the hydrogen bonding interactions between adjacent layers in **3**. The chains in adjacent layers have been coloured in blue and maroon to distinguish them from each other

Table 4.6. Hydrogen-bond geometry (Å, º) for **3**

X−H⋯A	X−H	H⋯A	X⋯A	∠(XHA)
O14−H14A⋯Cl1[i]	0.96	1.76	3.244(2)	178
N8−H8⋯Cl1[ii]	0.88	2.37	3.244(2)	174
O14−H14B⋯O12	0.96	1.73	2.718(3)	176
O13−H13A⋯O10[iii]	0.96	2.22	2.672(3)	166
O13−H13B⋯Cl1[iv]	0.96	2.19	3.180(2)	176
O12−H12A⋯Cl1[iii]	0.96	2.14	3.095(2)	174

Symmetry codes: (i) $-x+1$, $-y-1$, $-z$ (ii) $x-1$, y, $-z$ (iii) $-x+1$, $y+1/2$, $-z+1/2$ (iv) x, $-y-1/2$, $z+1/2$

4.2.1.4 {[Co(**FUM**)(H$_2$O)$_4$]·(Cl$_2$)·(H$_2$O)$_2$}$_n$ **4**

Crystals suitable for SCD analysis were grown by slow evaporation of a solution consisting of **FUM** and CoCl$_2$ in a M:L ratio of 1:4 in ethanol. The asymmetric unit (Figure 4.13) consists of half a **FUM** molecule, a cobalt cation with half occupancy, one chlorine anion, two coordinated water molecules and an uncoordinated water molecule. The metal centre adopts a distorted octahedral geometry (Table 4.7). The structure can be considered to be isostructural with the nickel complex described above, with unit cell dimensions approximately equal to those of the nickel complex. The hydrogen bonding pattern in the structure is the same as in the nickel complex and will not be discussed further. Hydrogen bonding details are given in Table 4.8.
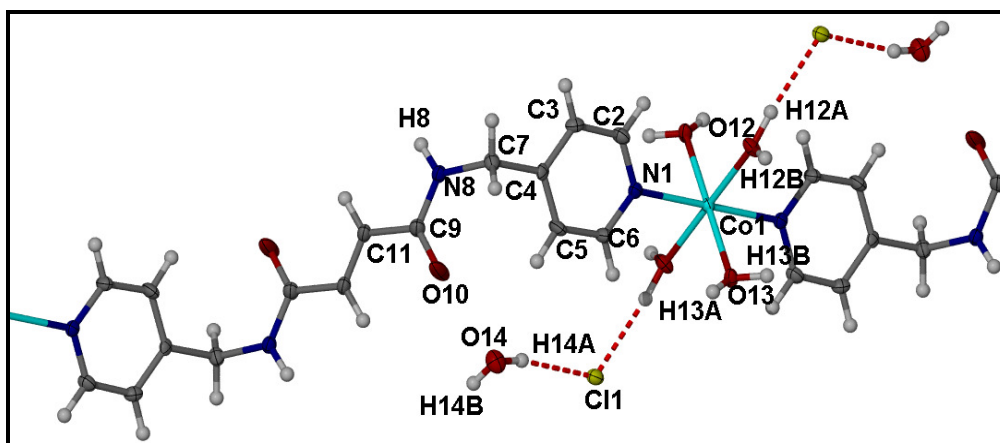
Figure 4.13. The molecular structure of **4** showing crystallographic labelling scheme and 50% probability ellipsoids for non-hydrogen atoms. Red dashed lines indicate hydrogen bonding.

Table 4.7. Coordination geometric parameters (Å, °) for **4**

Distance		Angle	
Co1$-$O12	2.072(2)	O12$-$Co1$-$O12^i	180.0(7)
Co1$-$O12^i	2.072(2)	O12$-$Co1$-$O13^i	88.5(7)
Co1$-$O13	2.117(2)	O12$-$Co1$-$O13	91.5(7)
Co1$-$O13^i	2.117(2)	O12$-$Co1$-$N1	88.5(8)
Co1$-$N1	2.130(2)	O12$-$Co1$-$N1^i	91.5(9)
Co1$-$N1^i	2.130(2)	O13$-$Co1$-$N1	90.4(7)
Angle		O13$-$Co1$-$N1^i	89.6(8)
O12^i$-$Co1$-$O13^i	91.5(8)	N1$-$Co1$-$N1^i	180.0(9)
O12^i$-$Co1$-$O13	88.5(7)		
O12^i$-$Co1$-$N1	91.5(9)		
O12^i$-$Co1$-$N1^i	88.5(8)		
O13^i$-$Co1$-$O13	180.0(9)		
O13^i$-$Co1$-$N1	89.6(8)		
O13^i$-$Co1$-$N1^i	90.4(7)		

Symmetry codes: (i) -*x*, -*y*+1, -*z*

Table 4.8. Hydrogen-bond geometry (Å, °) for **4**

X$-$H$\cdots$A	X$-$H	H$\cdots$A	X$\cdots$A	∠(XHA)
N8$-$H8$\cdots$Cl1^{ii}	0.88	2.37	3.246(3)	173
O13$-$H13A$\cdots$Cl1^{iii}	0.96	2.26	3.206(2)	173
O13$-$H13B$\cdots$O10^{vi}	0.96	1.77	2.678(4)	170
O14$-$H14A$\cdots$Cl1	0.97	2.19	3.101(2)	158
O12$-$H12A$\cdots$Cl1	0.97	2.18	3.142(3)	176
O12$-$H12B$\cdots$O14^v	0.97	1.73	2.625(4)	153
O14$-$H14B$\cdots$O14^{vi}	0.97	2.12	2.830(6)	129

Symmetry codes: (ii) -*x*-1, -*y*+1, -*z*, (iii) -*x*, *y*-1/2, -*z*+1/2, (vi) -*x*, *y*+1/2, -*z*+1/2, (v) -*x*, -*y*+3/2, *z*+1/2, (vi) -*x*, -*y*+2, -*z*

4.2.2 Crystal structures obtained with SUC

4.2.2.1 {[Co(**SUC**)(H$_2$O)$_4$]·(H$_2$O)$_2$·Cl$_2$]}$_n$ **5**

Crystals suitable for SCD analysis were grown by slow evaporation of an ethanolic solution of **SUC** and cobalt chloride in an M:L ratio of 1:4. The compound crystallizes in the monoclinic space group *P*2$_1$/*c*. The asymmetric unit (Figure 4.14) consists of half a **SUC** molecule, a cobalt cation at half occupancy, a chloride anion, two coordinated water molecules and an uncoordinated water molecule. The metal centre which is coordinated to two **SUC** molecules *via* the pyridyl nitrogen atom and also to four water molecules adopts an octahedral geometry (Table 4.9).
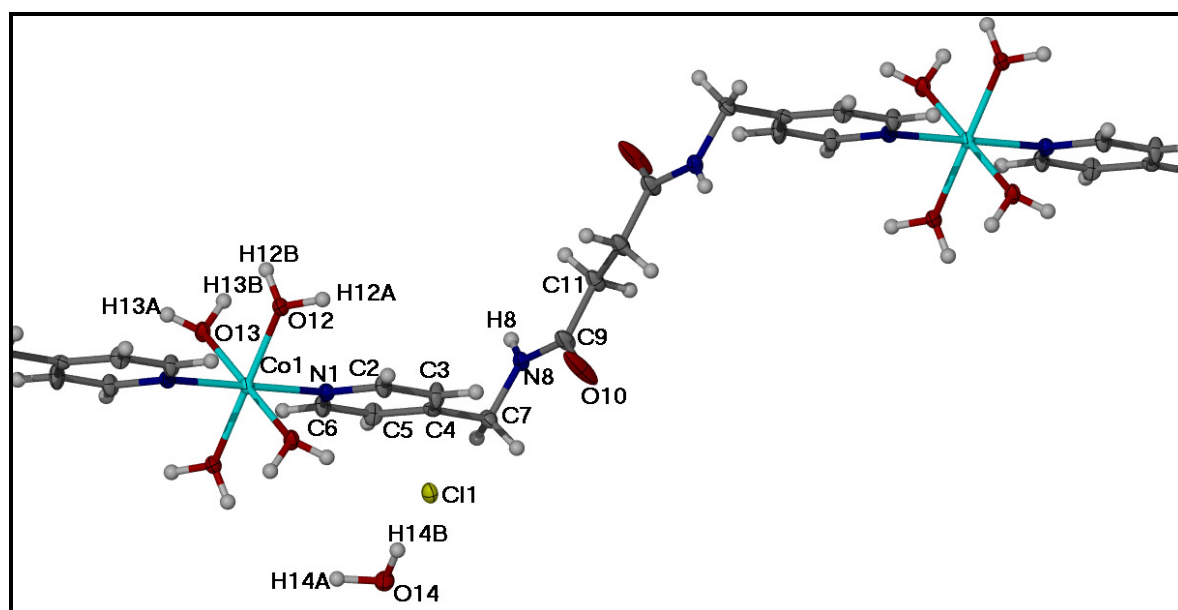
Figure 4.14. The molecular structure of **5** showing crystallographic labelling scheme and 50% probability ellipsoids for non-hydrogen atoms. Only the asymmetric unit is labelled.

Table 4.9. Coordination geometric parameters for (Å, °) **5**

Distance		Angle	
Co1−O12	2.085(2)	O12−Co1−O12^i	180.1(6)
Co1−O12^i	2.085(2)	O12−Co1−O13^i	88.9(6)
Co1−O13^i	2.121(2)	O12−Co1−O13	91.1(7)
Co1−O13	2.121(2)	O12−Co1−N1^i	91.8(8)
Co1−N1^i	2.123(2)	O12−Co1−N1	88.2(7)
Co1−N1	2.123(2)	O13−Co1−N1^i	89.7(7)
Angle		O13−Co1−N1	90.2(6)
O12^i−Co1−O13^i	91.1(7)	N1^i−Co1−N1	180.0
O12^i−Co1−O13	88.9(6)		
O12^i−Co1−N1^i	88.2(7)		
O12^i−Co1−N1	91.8(8)		
O13^i−Co1−O13	180.0(8)		
O13^i−Co1−N1^i	90.2(6)		
O13^i−Co1−N1	89.8(7)		

Symmetry codes: (i) -*x*+1, -*y*+1, -*z*

The hydrogen bonding pattern in the structure is identical to that of complex **3** and **4** and will therefore not be discussed further. Hydrogen bond details are given in Table 4.10.

Table 4.10. Hydrogen-bond geometry (Å, °) for **5**

X−H⋯A	X−H	H⋯A	X⋯A	∠(XHA)
N8−H8⋯Cl1[ii]	0.88	2.40	3.272(2)	173
O14−H14B⋯Cl1	0.96	2.15	3.106(2)	173
O13−H13A⋯Cl1	0.96	2.30	3.239(2)	168
O13−H13B⋯O10[iii]	0.95	1.78	2.676(3)	168
O12−H12B⋯O14[vi]	0.96	1.76	2.723(3)	177
O12−H12A⋯Cl1[v]	0.96	2.19	3.149(2)	175
O14−H14A⋯O14[vi]	0.96	1.92	2.847(4)	161

Symmetry codes: (ii) x-1, -y+1/2, z-1/2, (iii) -x+1, y+1/2, -z+1/2, (iv) -x+1, -y+1, -z+1, (v) -x+1, y+1/2, -z+1/2, (vi) -x+1, -y+1, -z+1

4.2.3 Comparison of complexes 1-5

A detailed comparison of complexes **1-5** is given in Table 4.11. In complexes **1-4** the ligand assumes an **S** conformation as in the reported pure **FUM** crystal structure.[1] The ligand comprises three planes, two planes are formed by the 4-(aminomethyl)pyridine, while the third plane is formed by the spacer atoms. It is interesting to note that none of these complexes display self-complementary amide hydrogen bonds between the **FUM** ligands even though they are found in the crystal structure of the pure ligand.[10] The amide group is involved in hydrogen bonding with the counter ions as well as the water molecules.

Complexes **1** and **2** were grown under identical crystallization conditions except that the counter ion in complex **1** is a sulphate while in complex **2** the counter ion is a nitrate. The counter ions in both complexes are non-coordinating, but the metal centres assume different coordination geometries, (trigonal bipyramidal for complex **1** and distorted octahedral for complex **2**). Both complexes consist of 1-D chains; the 1-D chains in complex **1** assume zigzag shape while those in complex **2** are undulating. The counter ions in both complexes assume the role of linking 1-D chains. The sulphate anion because of its shape further links the 1-D chains into a 3-D network, while the nitrate anions links the 1-D chains into a 2-D network.

It is interesting to compare complexes **4** and **5** since they are isostructural, but they were grown from different ligands. **SUC** and **FUM** differ in nature of the spacer unit; **FUM** consists of a *trans* C═C double bond, while that of **SUC** consists of C−C single bond. Despite this difference in the spacer unit the two ligands assume the same conformation and hence similar structures. Overall, all the complexes crystallize in the space group $P2_1/c$, with the structure consisting of two distinct layers that are arranged in a …ABABA… manner. The counter ions and water molecules play the role of linking lower dimension entities into higher dimension networks.[5]

Table 4.11. Comparison of complexes **1-5**

Complex	1	2	3-5
Space group	$P2_1/c$	$P2_1/c$	$P2_1/c$
Dimensionality	3-D hydrogen bonded network	2-D hydrogen bonded network	2-D hydrogen bonded network
Metal centre coordination geometry	Distorted trigonal bipyramidal	Distorted octahedral	Distorted octahedral
Ligand conformation	**S** shaped	**S** shape	**S** shape

4.2.4 Crystal structures obtained with ADI

4.2.4.1 $[Cd(ADI)_{1.5}(NO_3)_2]_n$ **6**

Crystals suitable for SCD analysis were grown by slow evaporation of an ethanolic solution of $Cd(NO_3)_2$ and **ADI** in a 1:1 molar ratio. The compound crystallizes in the triclinic space group $P\bar{1}$. The asymmetric unit (Figure 4.15) consists of three unique half **ADI** ligands, a Cd(II) cation and two nitrate anions. The Cd(II) centre, which adopts a pentagonal bipyramidal geometry is coordinated to three ligands *via* the pyridyl nitrogen atoms, one ligand *via* the amide carbonyl oxygen and two nitrate anions. One of the nitrate anions coordinates in a chelating fashion (bite angle 49.89º) while the other nitrate anion coordinates *via* one oxygen atom. Coordination geometric parameters are given in Table 4.12 and a perspective view of the coordination environment around the metal centres is shown in Figure 4.16.

Table 4.12. Coordination geometric parameters (Å, °) for **6**

Distance		Angle	
Cd1−N13	2.293(2)	N13−Cd1−N1	177.6(6)
Cd1−N1	2.293(2)	N13−Cd1−N25	95.1(7)
Cd1−N25	2.431(2)	N13−Cd1−O10^i	91.7(7)
Cd1−O10^i	2.434(2)	N13−Cd1−O39	81.4(8)
Cd1−O39	2.481(3)	N13−Cd1−O42	88.9(8)
Cd1−O42	2.490(2)	N13−Cd1−O38	90.0(7)
Cd1−O38	2.562(2)	N25−Cd1−O10^i	152.3(6)
Angle		N25−Cd1−O39	125.2(7)
N1−Cd1−N25	93.2(7)	N25−Cd1−O42	77.6(8)
N1−Cd1−O10^i	80.8(6)	N25−Cd1−O38	76.0(8)
N1−Cd1−O39	93.8(8)	O39−Cd1−O42	156.0(6)
N1−Cd1−O42	91.8(7)	O39−Cd1−O38	49.6(8)
N1−Cd1−O38	92.1(7)	O42−Cd1−O38	153.4(6)
O10^i−Cd1−O39	82.3(7)		
O10^i−Cd1−O42	75.6(6)		
O10^i−Cd1−O38	131.0(7)		

Symmetry codes (i) *-x, -y+1, -z*

Figure 4.15. The molecular structure of **6** showing 50% probability ellipsoids for non-hydrogen atoms. Only the asymmetric unit is labelled.

The structure consists of three independent ligands labelled **a**, **b** and **c** as shown in Figure 4.17. The metal centres are linked by alternating **a** and **b** ligands into a 1-D strand, with a Cd⋯Cd distance of approximately 22.45 Å along **a** and Cd⋯Cd distance of approximately 20.52 Å along **b**. Ligands **a** and **b** assume an elongated **S** shape, ligand **c** which links 1-D chains into a 2-D network is constrained into a more well-defined **S** shape to fit within a Cd⋯Cd distance of approximately 16.75 Å (Figure 4.17).

Figure 4.16. Coordination geometry around the Cd(II) centre in **6.**
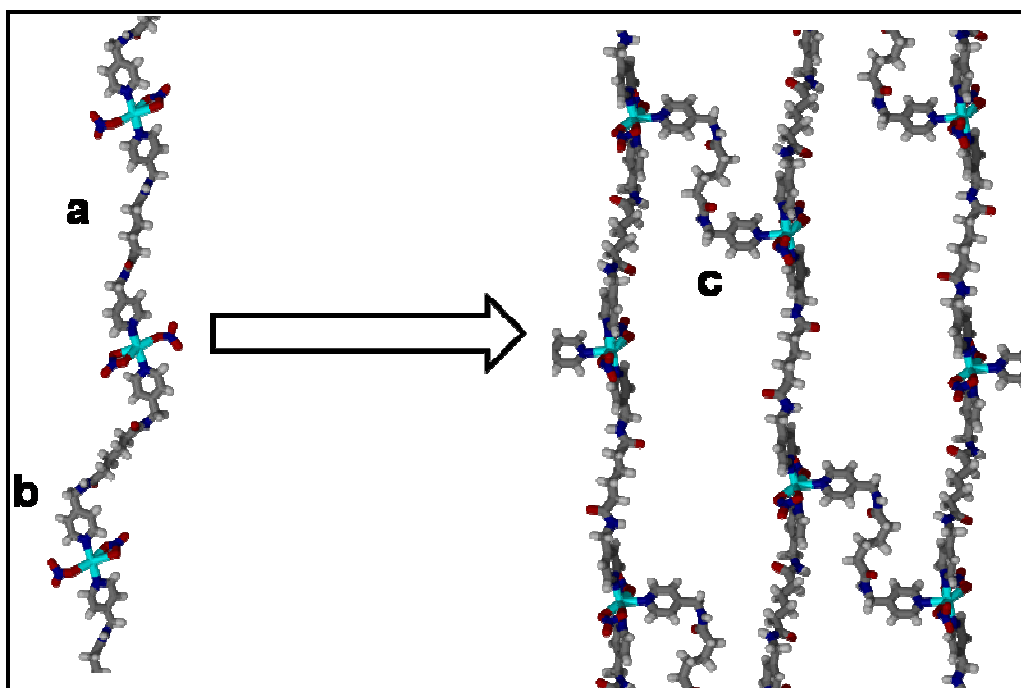
Figure 4.17. The 2-D network in **6** formed as a result of coordination bonds between the Cd(II) centre and the three independent ligands.

The packing can be described as four 2-D nets that stack on top of one another in an offset fashion. Owing to this staggered arrangement, the carbonyl oxygen of each chain points directly at the Cd(II) centre of its neighbour at a distance short enough for a coordination bond. The staggered arrangement is further stabilised by a self complementary amide hydrogen bond[11] (N8─H8····O22^v) (Figures 4.18 and 4.19). The 2-D nets assume a packing arrangement that occupies space such that no solvent molecules are included in the structure. All hydrogen bond details are given in Table 4.13.

Table 4.13. Hydrogen-bond geometry (Å, º) for **6**

X─H····A	X─H	H····A	X····A	∠(XHA)
N20─H20····O42^{ii}	0.88	2.36	3.173(3)	154
N20─H20····O44^{iii}	0.88	2.57	3.380(3)	153
N32─H32····O44^{vi}	0.88	2.62	3.216(3)	126
N8─H8····O22^v	0.88	1.93	2.788(3)	163

Symmetry codes: (ii) -x+1, -y, -z, (iii) -x+1, -y, -z, (vi) x, y-1, z, (v) x, y, z-1
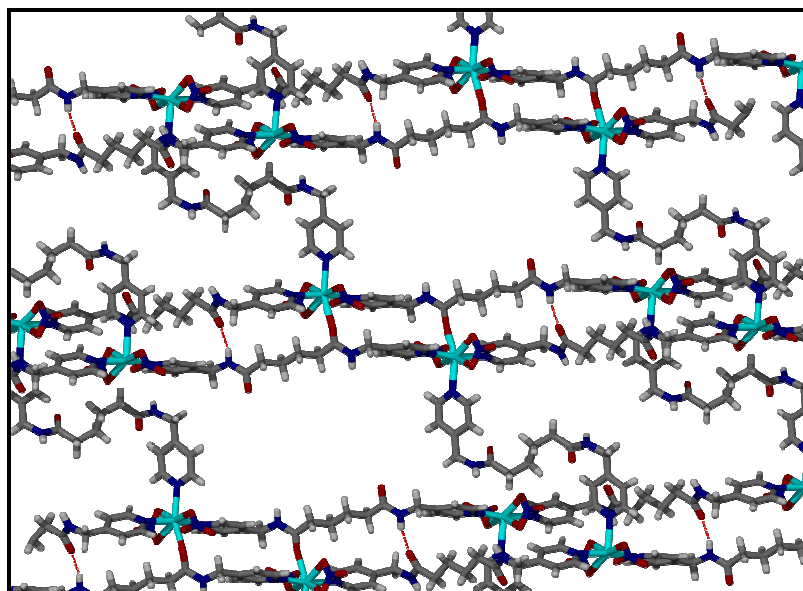
Figure 4.18. Capped stick representation of 2-D nets in **6**.The nets interact *via* a coordination bond between the amide carbonyl group as well as a self-complementary amide bond. The other two nets have been omitted for clarity.
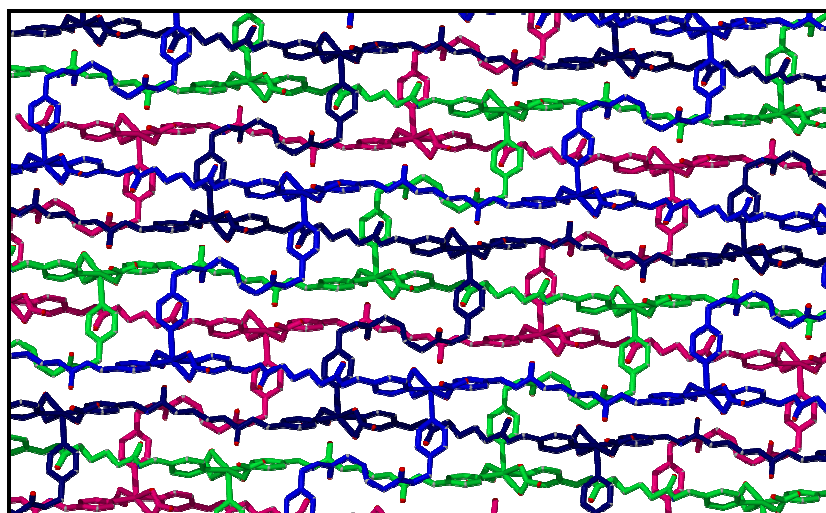

Figure 4.19. The packing diagram of **6** showing all four 2-D nets. The nets have been coloured in four different colours to distinguish them from one another. The hydrogen bonding and the coordination bonds have been omitted for clarity.

4.2.4.2 {[Zn$_2$(**ADI**))(H$_2$O)$_5$]·(NO$_3$)·(H$_2$O)$_2$}$_n$ **7**
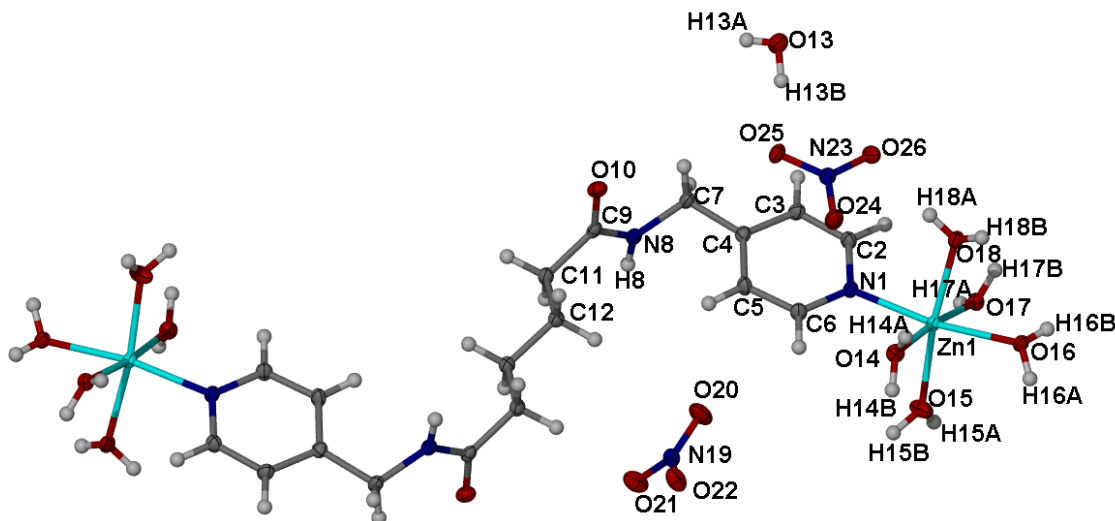

Figure 4.20. The molecular structure of **7** showing the crystallographic labelling scheme and 50% probability ellipsoids for non-hydrogen atoms. Only the asymmetric unit is labelled.

Single crystals suitable for SCD analysis were grown by slow evaporation of a solution of **ADI** and Zn(NO$_3$)$_2$ in a M:L ratio of 1:2 in ethanol. The compound crystallizes in the monoclinic space group *P*2$_1$/*c*. The asymmetric unit, (Figure 4.20), consists of half an **ADI** molecule, five coordinated water molecules, two nitrate anions, a Zn(II) cation and one uncoordinated water molecule. The Zn(II) cation is in an octahedral environment, with four equatorial positions occupied by water molecules and two axial positions occupied by a water molecule and an **ADI** molecule. Coordination geometric parameters are given in Table 4.14. The metal centres are connected by a single bridging ligand to form a discrete **S** shaped unit.

Figure 4.21 shows the packing diagram of complex **7** with the **S** shaped units arranged in diagonal columns which are parallel to the *bc* plane. The **S** shaped units in one column are related to each other by a glide plane, and they are related to those in a column below by an inversion centre. One of the nitrate anions and the uncoordinated water molecules are located between the columns. The region within the ellipse in Figure 4.21, when viewed along [-101] (Figure 4.22), shows that the coordinated water molecule of each **S** shaped unit points towards the amide oxygen of the neighbouring unit, at a distance short enough for a hydrogen bond (O16−H16A⸺O10[viii]). Owing to this interaction, a continuous 1-D looped chain is formed, which is linked to another 1-D chain below *via* a hydrogen bonding interaction between a coordinated water molecule and a nitrate anion (O18−H18A⸺O26 and O17−H17B⸺O26[iii]), to form 2-D network. The nitrate anion is also hydrogen bonded to the uncoordinated water molecule (O13−H13B⸺O25) which, in turn, accepts a hydrogen bond from a coordinated water molecule (O16−H16B⸺O13[x]).

Table 4.14. Coordination geometric parameters (Å, º) for **7**

Distance		Angle	
Zn1−O15	2.0631(1)	O15−Zn1−O14	85.1(7)
Zn1−O14	2.093(1)	O15−Zn1−O18	172.9(6)
Zn1−O18	2.094(1)	O15−Zn1−O17	89.8(2)
Zn1−O17	2.096(1)	O15−Zn1−ON1	97.1(7)
Zn1−N1	2.119(2)	O15−Zn1−O16	91.9(7)
Zn1−O16	2.151(1)	O17−Zn1−N1	94.4(5)
Angle		O17−Zn1−O16	85.0(5)
O14−Zn1−O18	94.9(7)	N1−Zn1−O16	170.9(5)
O14−Zn1−O17	174.1(5)		
O14−Zn1−N1	91.1(5)		
O14−Zn1−O18	91.2(5)		
O18−Zn1−O17	89.3(5)		
O18−Zn1−N1	90.0(7)		
O18−Zn1−O16	81.1(5)		
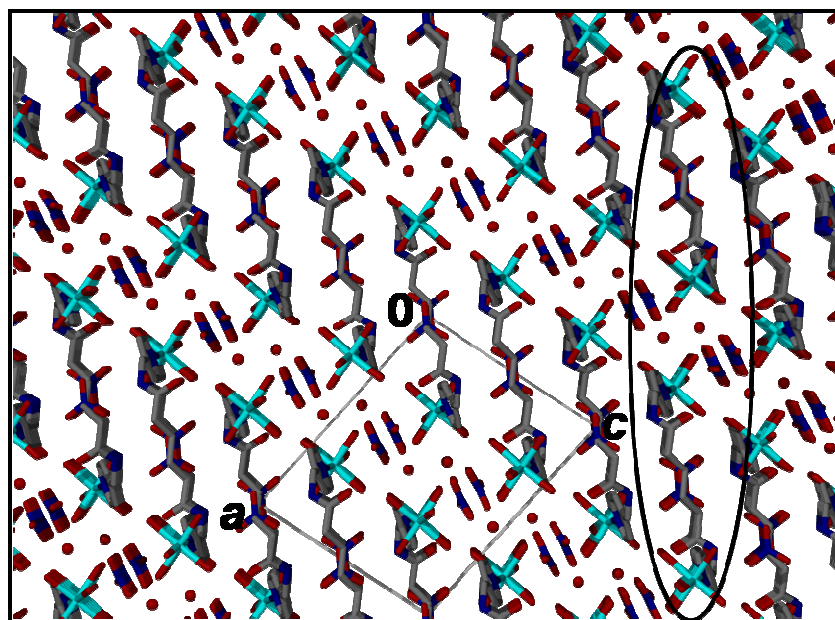
Figure 4.21. The packing diagram of **7** viewed along [010]. The region within the ellipse is shown magnified in Figure 4.22.
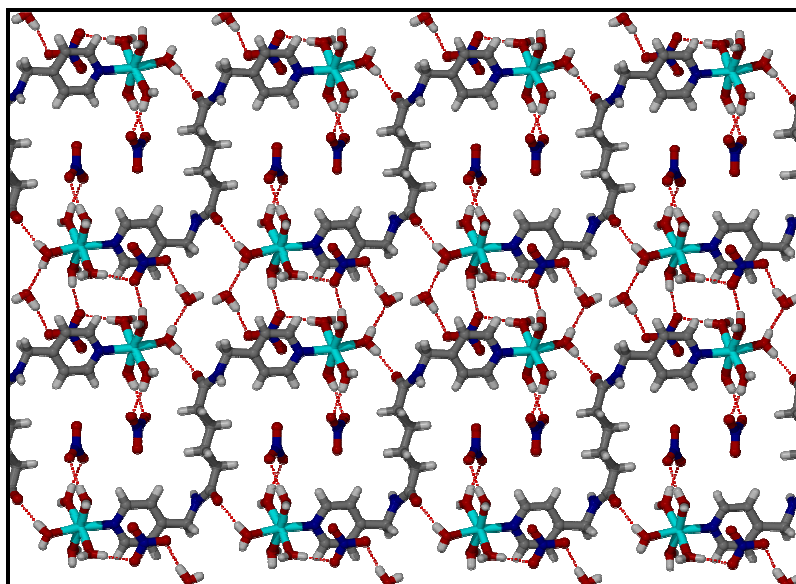
Figure 4.22. 2-D network formed as a result of hydrogen bonding interactions between **S** shaped units in **7** as viewed along [-101].

Finally, the **S** shaped units in the same column interact *via* six types of hydrogen bonds, four of these link the units *via* a nitrate anion (O14−H14B····O21^{vii}, O15−H15A····O21^{vi}, N8−H8····O22^{i}, O15−H15B····O22^{ii}) and a single hydrogen bond links the chains *via* an uncoordinated water molecule (O14−H14A····O13^{v}). The sixth hydrogen bond is a direct interaction between a coordinated water molecule and amide oxygen (O17−H17A····O10^{iv}). These hydrogen bonding interactions further link the 2-D into a 3-D network. Details of hydrogen bonding are given in Table 4.15.

Table 4.15. Hydrogen-bond geometry (Å, °) for **7**

X−H····A	X−H	H····A	X····A	∠(XHA)
N8−H8····O22^{i}	0.88	1.98	2.840	167
O15−H15B····O22^{ii}	0.96	1.76	2.719(2)	172
O17−H17B····O26^{iii}	0.96	1.83	2.787(2)	176
O17−H17A····O10^{iv}	0.96	2.01	2.706(2)	176
O14−H14A····O13^{v}	0.96	1.87	2.805(2)	165
O15−H15A····O21^{vi}	0.96	1.76	2.674(2)	158
O14−H14B····O21^{vii}	0.96	1.84	2.788(2)	169
O13−H13B····O25	0.96	1.85	2.798(2)	167
O16−H16A····O10^{viii}	0.96	1.81	2.764(2)	171
O18−H18B····O25^{ix}	0.96	1.85	2.785(2)	166
O16−H16B····O13^{x}	0.96	1.89	2.845(2)	173
O18−H18A····O26	0.96	1.78	2.735(2)	175
O13−H13A····O24^{xi}	0.96	2.09	2.903(2)	142

Symmetry codes: (i) *x*, -*y*+1/2, *z*-1/2, (ii) -*x*+2, -*y*+1, -*z*+1, (iii) -*x*+1, -*y*+1, -*z*, (iv) *x*, -*y*+1/2, *z*-1/2, (v) -*x*+1, *y*+1/2, -*z*+1/2, (vi) -*x*+2, *y*+1/2, -*z*+1/2, (vii) -*x*+2, -*y*+1, -*z*+1, (viii) *x*, *y*+1, *z*, (ix) -*x*+1, *y*+1/2, -*z*+1/2, (x) -*x*+1, -*y*+1, -*z*, (xi) -*x*+1,*y*-1/2, -*z*+1/2

4.2.4.3 $\{[Zn(\mathbf{ADI})(H_2O)_4]\cdot(NO_3)_2\cdot(H_2O)_2\}_n$ **8**, $\{[Cd(\mathbf{ADI})(H_2O)_4]\cdot(NO_3)_2\cdot(H_2O)_2\}_n$ **9** $\{[Cu(\mathbf{ADI})(H_2O)_4]\cdot(NO_3)_2\cdot(H_2O)_2\}_n$ **10**

This section describes the structures of crystals obtained by slow evaporation of an ethanolic solution of $Zn(NO_3)_2$ and **ADI** (2:1 ratio), $Cd(NO_3)_2$ and **ADI** (1:2 ratio), $Cu(NO_3)_2$ and **ADI** (2:1 ratio). The three structures are isostructural. The asymmetric units (Figures 4.23-4.25) consist of half an **ADI** molecule, one nitrate anion, half a metal cation (M), two coordinated water molecules and an uncoordinated water molecule. The M(II) centre, which is coordinated to two water molecules and two ligands *via* the pyridyl nitrogen atom adopts a distorted octahedral geometry. Coordination geometric parameters for each complex are given in Tables 4.16, 4.18 and 4.20.
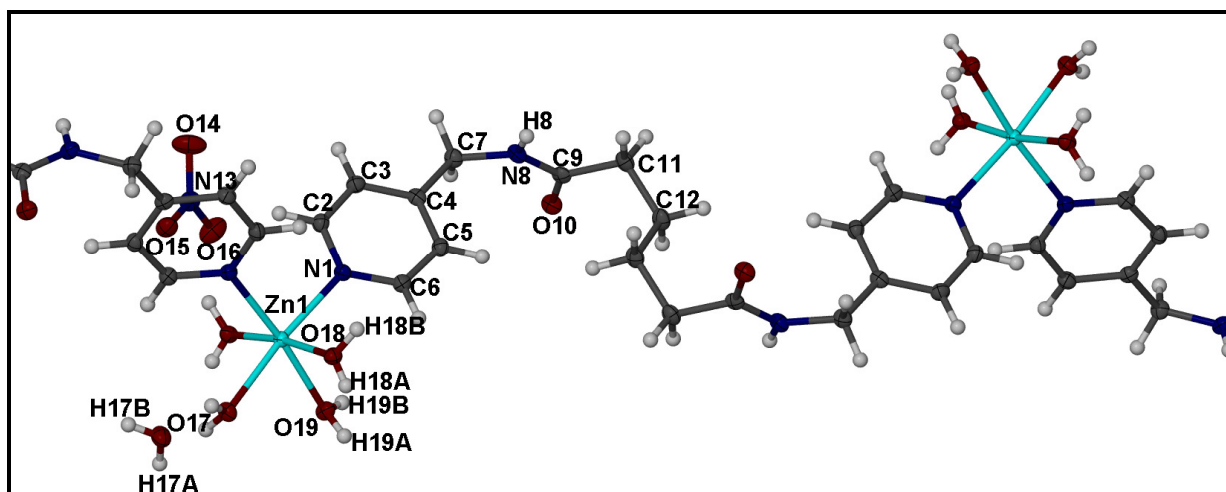

Figure 4.23. The molecular structure of **8** showing the crystallographic labelling scheme and 50% probability ellipsoids for non-hydrogen atoms. Only the asymmetric unit is labelled
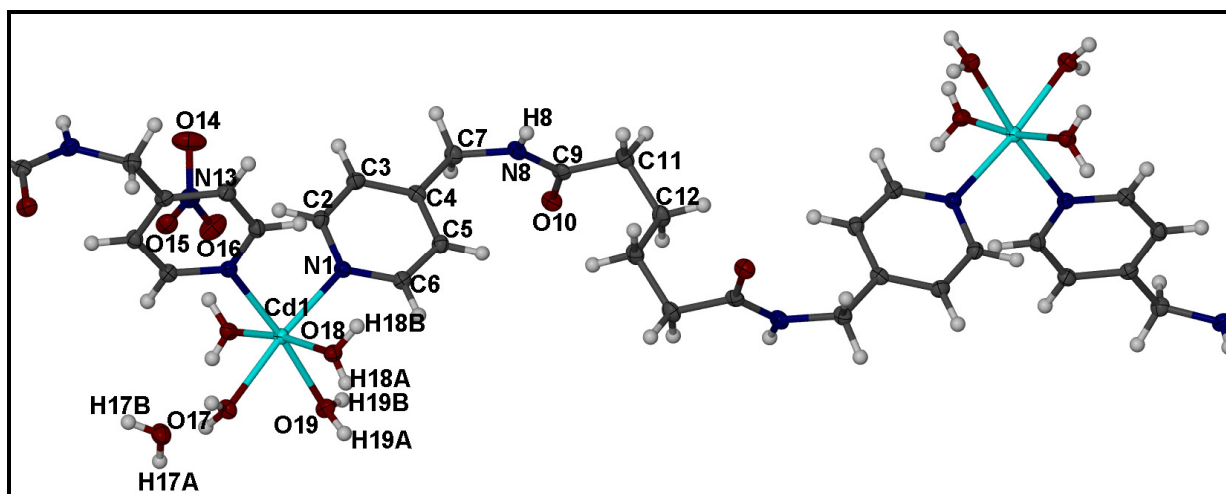

Figure 4.24. The molecular structure of **9** showing the crystallographic labelling scheme and 50% probability for non-hydrogen atoms. Only the asymmetric unit is labelled**.**
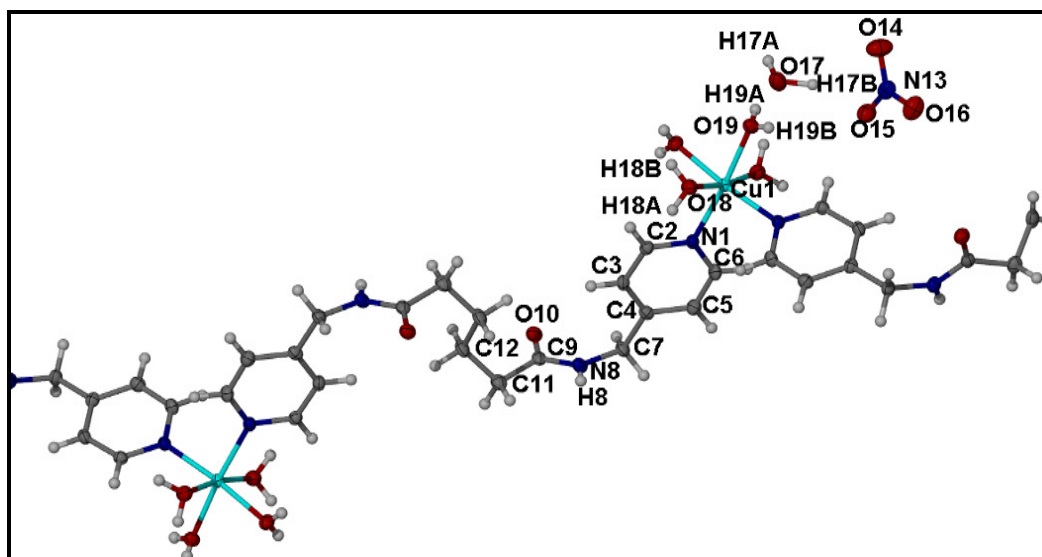
Figure 4.25. The molecular structure of **10** showing the crystallographic labelling scheme and 50% probability ellipsoids for non-hydrogen atoms. Only the asymmetric unit is labelled.

Table 4.16. Coordination geometric parameters (Å, °) for **8**

Distance		Angle	
Zn1−O18	2.097(1)	O18−Zn1−O18^i	172.7(6)
Zn1−O18^i	2.097(1)	O18−Zn1−O19	83.9(4)
Zn1−O19	2.122(1)	O18−Zn1−O19^i	90.6(4)
Zn1−O19^i	2.122(1)	O18−Zn1−N1^i	91.4(4)
Zn1−N1^i	2.142(1)	O18−Zn1−N1	93.7(4)
Zn1−N1	2.142(1)	O19^i−Zn1−N1^i	173.4(4)
Angle		O19^i−Zn1−N1	92.9(4)
O18^i−Zn1−O19	90.6(4)	N1^i−Zn1−N1	92.3(6)
O18^i−Zn1−O19^i	83.9(9)		
O18^i−Zn1−N1^i	93.7(4)		
O18^i−Zn1−N1	91.4(4)		
O19−Zn1−O19^i	82.0(6)		
O19−Zn1−N1^i	92.9(4)		
O19−Zn1−N1	174.3(4)		

Symmetry codes: (i) -*x*, -*y*-1, -*z*+2

In all the three complexes the metal centres are connected by a single bridging ligand to form 1-D polymeric chains in the [-101] direction. The ligand assumes an **S** shape in all three complexes with M⋯M distances ranging from 17.25 to 17.82 Å. Hydrogen bond interactions between the amide NH moiety and nitrate anion (N8−H8⋯O14^i), and between the amide carbonyl moiety and a coordinated water molecule (O19−H19B⋯O10^{iv}) constrain the ligand into an **S** shape. The same coordinated water molecule forms a second hydrogen bond to the uncoordinated water molecule (O19−H19B⋯O17). The remaining coordinated water molecule donates a hydrogen bond to the uncoordinated water molecule (O18−H18B⋯O17) and a nitrate anion (O18−H18A⋯O15). The uncoordinated water molecule in turn donates two hydrogen bonds to a nitrate anion (O17−H17A⋯O15^{ii} and O17H-17B⋯O14^v). This hydrogen bonding motif results in connection of the parallel 1-D chains into a 2-D network.

Details of hydrogen bonding for each complex are given in Tables 4.17, 4.19 and 4.21. The hydrogen bonding interactions between the 1-D chains is shown in Figure 4.26 and the packing diagram is shown in Figure 4.27

Table 4.17. Hydrogen-bond geometry (Å, º) for **8**

X−H····A	X−H	H····A	X−A	∠(XHA)
N8−H8····O14^i	0.88	2.00	2.857(2)	163
O18−H18B····O17	0.96	1.77	2.710(2)	167
O18−H18A····O15	0.96	1.82	2.771(2)	172
O18−H18A····O15	0.96	1.82	2.771(2)	172
O17−H17A····O15^{ii}	0.96	1.89	2.786(2)	155
O19−H19B····O17^{iii}	0.96	1.97	2.851(2)	153
O19−H19A····O10^{iv}	0.96	1.74	2.700(1)	177
O17−H17B····O14^{v}	0.96	1.83	2.782(2)	177

Symmetry codes: (i) -x, -y-1, -z+2, (ii) -x, -y, -z+2, (iii) -x, y, -z+3/2, (iv) x+1/2, y+1/2, z, (iv) x, y+1, z
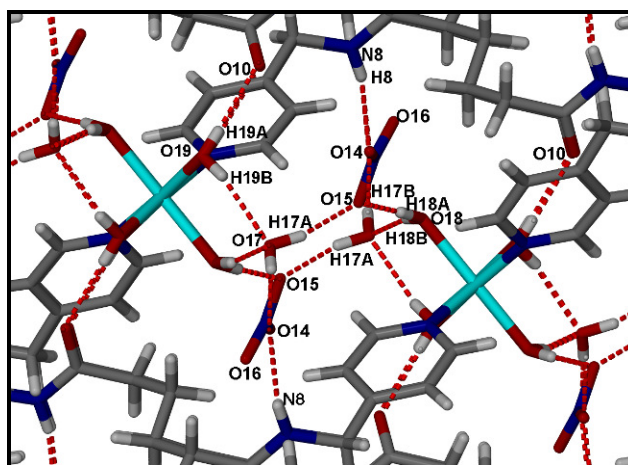

Figure 4.26. Capped stick representation of the hydrogen bonding interaction between 1-D chains in **8**-**10**. The 1-D chains are linked *via* the nitrate anion and the water molecule into a 2-D network.

Table 4.18. Coordination geometric parameters (Å, º) for **9**

Distance		Angle	
Cd1−O18	2.287(1)	O18−Cd1−O18^i	172.1(8)
Cd1−O18^i	2.287(1)	O18−Cd1−O19	84.1(6)
Cd1−O19	2.298(1)	O18−Cd1−O19^i	90.0(5)
Cd1−O19^i	2.298(1)	O18−Cd1−N1	94.0(5)
Cd1−N1	2.327(1)	O18−Cd1−N1^i	94.4(5)
Cd1−N1^i	2.327(1)	O19^i−Cd1−N1	92.9(6)
Angle		O19^i−Cd1−N1^i	175.3(5)
O18^i−Cd1−O19	90.0(5)	N1−Cd1−N1^i	91.5(7)
O18^i−Cd1−O19^i	84.1(5)		
O18^i−Cd1−N1	91.4(5)		
O18^i−Cd1−N1^i	94.1(5)		
O19−Cd1−O19^i	82.8(7)		
O19−Cd1−N1	175.3(4)		
O19−Cd1−N1^i	92.9(5)		

Symmetry codes: (i) -x, -y+2, -x+1

Table 4.19. Hydrogen-bond geometry (Å, °) for **9**

X−H····A	X−H	H····A	X····A	∠(XHA)
N8−H8····O14[i]	0.88	2.01	2.852(2)	159
O18−H18B····O17	0.96	1.76	2.705(2)	170
O17−H17B····O15[ii]	0.96	1.89	2.780(2)	154
O17−H17B····N13[ii]	0.96	2.59	3.449(2)	150
O18−H18A····O15	0.96	1.84	2.778(2)	167
O17−H17A····O14[iii]	0.96	1.82	2.778(2)	174
O19−H19A····O17[iv]	0.96	1.95	2.842(2)	154
O19−H19B····O10[v]	0.96	1.74	2.703(2)	179

Symmetry codes: (i) -*x*, -*y*+2, -*x*+1, (ii) -*x*, -*y*+1, -*z*+1, (iii) *x*, *y*-1, *z*, (iv) -*x*, *y*, -*z*+3/2, (v) *x*-1/2, *y*-1/2, *z*

Table 4.20. Coordination geometric parameters (Å, °) for **10**

Distance		Angle	
Cu1−O19	2.004(3)	O19−Cu1−O19[i]	82.8(8)
Cu1−O19[i]	2.004(3)	O19−Cu1−N1	174.8(2)
Cu1−N1	2.018(3)	O19−Cu1−N1[i]	92.6(1)
Cu1−N1[i]	2.018(3)	O19−Cu1−O18	83.3(1)
Cu1−O18	2.304(3)	O19−Cu1−O18[i]	90.9(1)
Cu1−O18[i]	2.304(3)	N1−Cu1−O18	91.0(1)
Angle		N1−Cu1−O18[i]	94.3(1)
O19[i]−Cu1−N1	92.6(1)	O18−Cu1−O18[i]	172.2(2)
O19[i]−Cu1−N1[i]	174.8(1)		
O19[i]−Cu1−O18	90.9(1)		
O19[i]−Cu1−O18[i]	83.3(1)		
N1−Cu1−N1[i]	92.1(2)		
N1−Cu1−O18	94.3(1)		
N1−Cu1−O18[i]	91.1(1)		

Symmetry codes: (i) -*x*+1, *y*, -*z*+3/2

Table 4.21. Hydrogen-bond geometry (Å, °) for **10**

X−H····A	X−H	H····A	X····A	∠(XHA)
O18−H18B····O17[i]	0.96	1.99	2.857(4)	168.
O17−H17B····O15[i]	0.96	1.83	2.751(4)	160
O17−H17B····N13[i]	0.96	1.86	2.774(4)	158
N8−H8····O14[ii]	0.88	2.51	3.421(4)	158
O17−H17B····O14	0.96	2.58	3.380(4)	141
O19−H19A····O17[iii]	0.96	1.89	2.807(4)	159
O19−H19B····O10[iv]	0.96	1.71	2.655(3)	166
O18−H18A····O15[v]	0.96	1.91	2.794(4)	153
O18−H18A····N13[v]	0.96	2.55	3.341(4)	139
O18−H18A····O16[v]	0.96	2.59	3.230(4)	124
O17−H17A····O14[vi]	0.96	1.82	2.775(4)	173

Symmetry codes: (i) -*x*+1, *y*, -*z*+3/2, (ii) -*x*+1, *y*, -*z*+3/2, (iii) -*x*+1, *y*, -*z*+3/2, (iv) *x*+1/2, *y*+1/2, *z*, (v) *x*, -*y*+1, *z*+1/2, (vi) *x*, -*y*+2, *z*+1/2
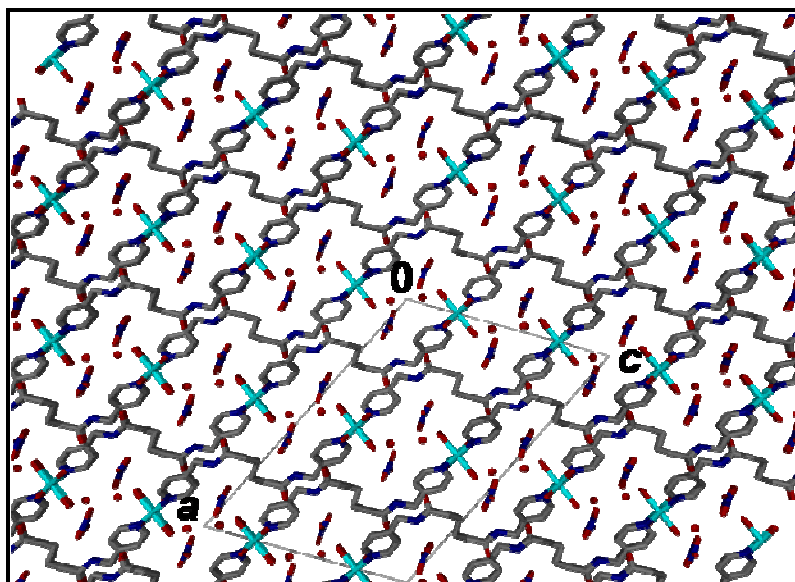
Figure 4.27. The packing diagram of complexes **8-10** viewed along [010]. The hydrogen atoms have been omitted for clarity.

4.2.4.4 {[Co(**ADI**)(H$_2$O)$_4$]·(H$_2$O)$_2$·Cl$_2$}$_n$**11**
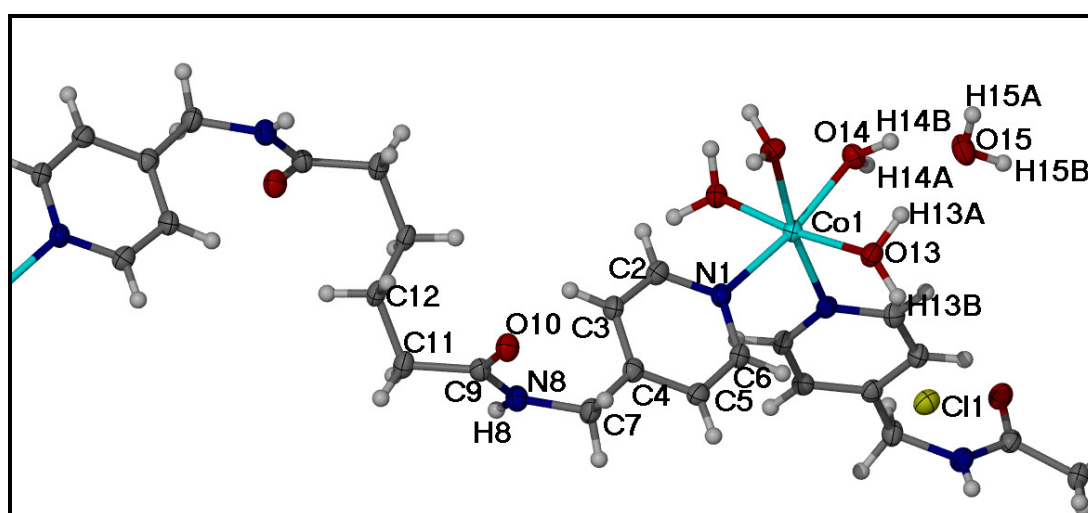

Figure 4.28. The asymmetric unit of **11** showing the crystallographic labelling scheme and 50% probability ellipsoids for non-hydrogen atoms. Only the asymmetric unit is labelled.

Crystals suitable for SCD analysis were grown by slow evaporation of an ethanolic solution of CoCl$_2$ and **ADI**. The compound crystallizes in the monoclinic space group *C*2/*c*. The asymmetric unit (Figure 4.28) consists of half an **ADI** molecule, half a cobalt cation, a chloride anion, two coordinated water molecules and one uncoordinated water molecule. The metal centre, which is coordinated to two **ADI** molecules *via* the pyridyl nitrogen atom and four water molecules, adopts a distorted octahedral geometry, coordination parameters are given in Table 4.22. A single **ADI** molecule links metal centres to form continuous 1-D chains running along the crystallographic *b* axis. The ligand, as in the case of complexes **8**-**10**, adopts a

slightly elongated **S** shape, with a Co⸱⸱⸱⸱Co distance of 17.87 Å. The structure packs (Figure 4.29) in a fashion similar to that of the three nitrate complexes described above, with the chloride anions assuming the role of nitrate anions.
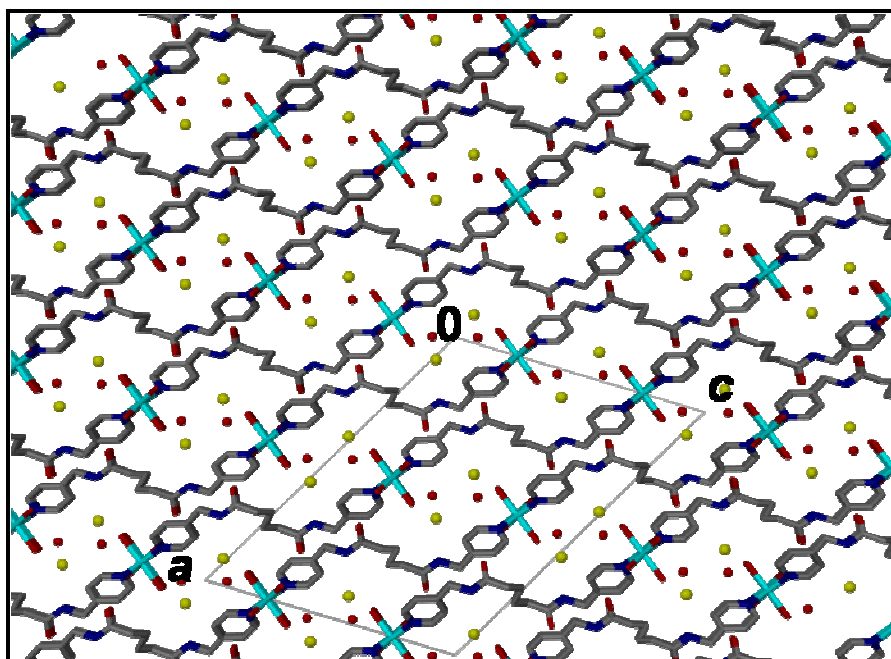

Figure 4.29. The packing diagram of **11** viewed along [010]. The hydrogen atoms have been omitted for clarity.

The 1-D chains interact *via* seven types of hydrogen bonds, with six of these linking the chains *via* the chloride anion. The uncoordinated water molecule accepts two hydrogen bonds from two coordinated water molecules of one chain (O14−H14B⸱⸱⸱⸱O15 and O13-H13A⸱⸱⸱⸱O15). The uncoordinated water molecule in turn donates two hydrogen bonds to two chloride anions, (O15−H15B⸱⸱⸱⸱Cl1^{iii} and O15−H15A⸱⸱⸱⸱Cl1^{vi}) which in turn accept two hydrogen bonds from an amide NH group of another chain as well as an uncoordinated water molecule (N8−H8⸱⸱⸱⸱Cl1^{ii} and O15−H15B⸱⸱⸱⸱Cl1^{iii}). The chlorine atom also accepts a third hydrogen bond from a coordinated water molecule (O13−H13B⸱⸱⸱⸱Cl1). The 1-D chains are also linked *via* a direct interaction between a coordinated water molecule of a chain and an amide oxygen of the neighbouring chain (O14−H14A⸱⸱⸱⸱O10^{vi}). This hydrogen bond interaction between 1-D chains is illustrated in Figure 4.30 and it results in a 2-D network. All hydrogen bonding details are given in Table 4.23.

Table 4.22. Coordination geometric parameters (Å, º) for **11**

Distance		Angle	
Co1 − O14^i	2.098(3)	O14^i − Co1 − O14	81.6(1)
Co1 − O14	2.098(3)	O14^i − Co1 − O13^i	90.9(1)
Co1 − O13^i	2,115(3)	O14^i − Co1 − O13	84.2(1)
Co1 − O13	2.115(3)	O14^i − Co1 − N1	91.8(1)
Co1 − NI	2.132(3)	O14^i − Co1 − N1^i	172.0(1)
Co1 − N1^i	2.132(3)	O13 − Co1 − N1	92.9(1)
Angle		O13 − Co1 − N1^i	91.5(1)
O14 − Cu1 − O13^i	84.2(1)	N1 − Co1 − N1^i	95.2(2)
O14 − Cu1 − O13	90.9(1)		
O14 − Cu1 − N1	172.0(1)		
O14 − Cu1 − N1^i	91.8(1)		
O13^i − Co1 − O13	173.2(2)		
O13^i − Co1 − N1	91.5(1)		
O13^i − Co1 − N1^i	92.9(1)		

Symmetry codes: (i) -x+1, y, -z+1/2
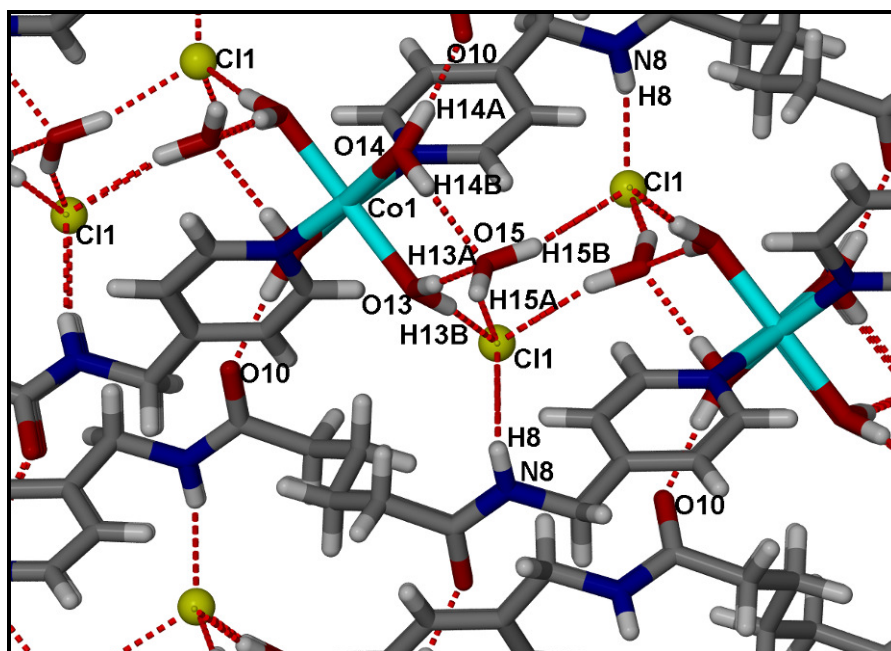
Figure 4.30. An expansion of the hydrogen bonding interactions between the 1-D chains in **11**.

Table 4.23. Hydrogen-bond geometry (Å, º) for **11**

X − H ⋯ A	X − H	H ⋯ A	X ⋯ A	∠(XHA)
N8 − H8 ⋯ Cl1^{ii}	0.86	2.39	3.239(3)	168.
O14 − H14B ⋯ O15	0.96	1.90	2.816(4)	158
O13 − H13A ⋯ O15	0.96	1.82	2.772(4)	169
O15 − H15B ⋯ Cl1^{iii}	0.96	2.19	3.145(3)	168
O13 − H13B ⋯ Cl1	0.96	2.16	3.101(3)	165
O15 − H15A ⋯ Cl1^{iv}	0.96	2.28	3.211(3)	161
O14 − H14A ⋯ O10^v	0.96	1.71	2.675(3)	176

Symmetry codes: (ii) x, -y+2, z-1/2 (ii) -x+1, -y+1, -z+1, (vi) x, y-1, z, (v) x-1/2, y-1/2, z

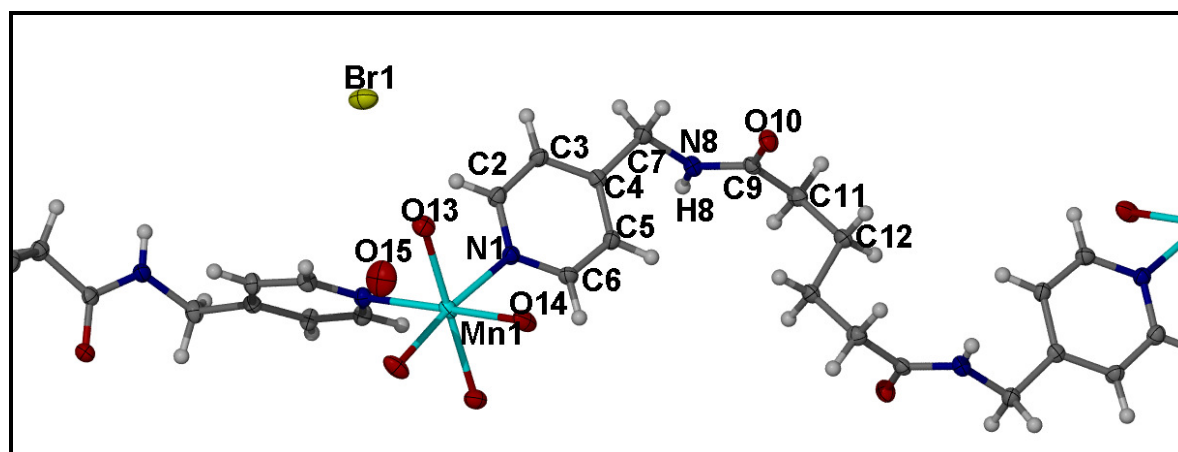**4.2.4.5** {[Mn(**ADI**)(H$_2$O)$_4$]·(Br$_2$)·(H$_2$O)$_2$}$_n$ **12**

Figure 4.31. The molecular structure of **11** showing the crystallographic labelling scheme and 50% probability ellipsoids for non-hydrogen atoms. Only the asymmetric unit is labelled.

Crystals suitable for SCD analysis were grown by slow evaporation of an ethanolic solution of **ADI** and MnBr$_2$ in a M:L ratio of 1:2. The compound crystallizes in the monoclinic space group *C*2/*c* with half an **ADI** molecule, a manganese cation at half occupancy, two coordinated water molecules and one uncoordinated water molecule in the asymmetric unit (Figure 4.31). The metal centre is coordinated to two ligands *via* the pyridyl nitrogen atoms and also to four water molecules. Coordination geometric parameters are given in Table 4.24. The structure is isostructural to that of complex **11** and hence no further crystal structure description is necessary. The packing diagram is identical to that of complex **11** (Figure 4.29).

Table 4.24. Coordination geometric parameters (Å, °) for **12**

Distance		Angle	
Mn1$-$O14^i	2.179(3)	O14^i$-$Mn1$-$O14	83.8(2)
Mn1$-$O14	2.179(3)	O14^i$-$Mn1$-$O13^i	84.8(2)
Mn1$-$O13^i	2.208(3)	O14^i$-$Mn1$-$O13	88.8(1)
Mn1$-$O13	2.208(3)	O14^i$-$Mn1$-$N1	173.8(2)
Mn1$-$NI	2.240(4)	O14^i$-$Mn1$-$N1^i	94.0(1)
Mn1$-$N1^i	2.240(4)	O13$-$Mn1$-$N1	94.3(1)
Angle		O13$-$Mn1$-$N1^i	91.8(1)
O14$-$Mn1$-$O13^i	84.4(1)	N1$-$Mn1$-$N1^i	94.5(2)
O14$-$Mn1$-$O13	84.8(1)		
O14$-$Mn1$-$N1	90.0(1)		
O14$-$Mn1$-$N1^i	173.8(2)		
O13^i$-$Mn1$-$O13	171.0(2)		
O13^i$-$Mn1$-$N1	91.8(1)		
O13^i$-$Mn1$-$N1^i	94.3(1)		

Symmetry codes: (i) *-x*+1, *y*, *-z*+1/2

4.2.4.6 Crystal structure obtained from **ADI** and trimesic acid **13**

A mixture of **ADI** and trimesic acid and a few drops of ethanol were ground using a mortar and pestle. The resulting paste was dissolved in water and the solvent was then allowed to evaporate. Crystals suitable for SCD analysis were obtained after several days. The compound crystallizes in the monoclinic space group $P2_1/n$ with one trimesic acid molecule and two halves of two unique **ADI** ligands in the asymmetric unit (Figure 4.32). The independent ligands have been labelled 13(a) and 13(b) in Table 4.26; 13(a) assumes a more well-defined **S** shape while 13 (b) assumes a somewhat stretched **S** shape. Five types of hydrogen bonds are encountered in the crystal structure. Four of these are hydrogen bonding interactions between the **ADI** ligand and the trimesic acid molecule (N8C—H8C⋯O1B, O1A—H1A⋯N1C[ii], O5A—H5A⋯N1B and O8A—H8A⋯O10B[iii]). These hydrogen bonding interactions result in a 2-D sheet shown in Figure 4.33. The fifth type of hydrogen bond is a self-complementary hydrogen bond between two entwined **ADI** molecules[11] (N8B—H8B⋯O10C[i]). Finally, the **ADI** and the trimesic acid molecules also interact *via* weak π-π interactions as evidenced by a centroid-to-centroid distance of 3.707 Å. The packing diagram is given in Figure 4.34.
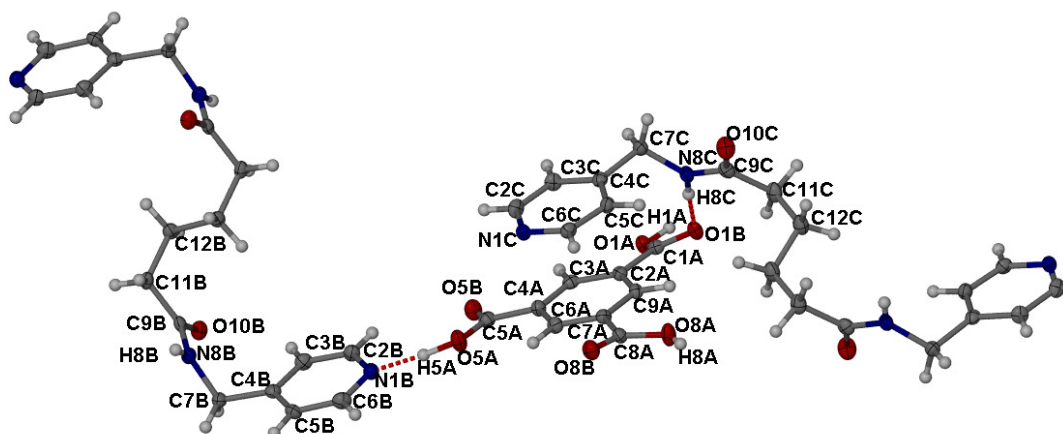

Figure 4.32. The molecular structure of **13** showing the crystallographic labelling scheme for the asymmetric unit and 50% probability ellipsoids for non-hydrogen atoms.
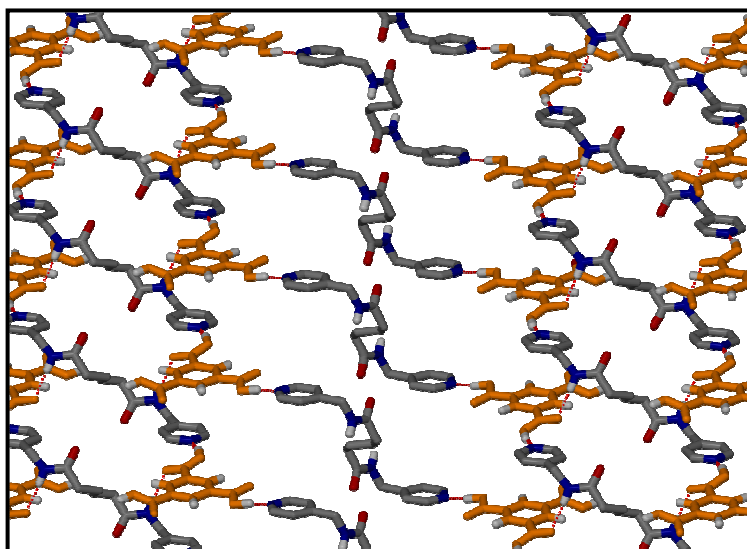
Figure 4.33. A 2-D sheet formed as a result of hydrogen bond interaction and π-π interactions between trimesic acid and **ADI** in **13.**

It is also interesting to note that in the presence of trimesic acid, the self-complementary amide hydrogen bonds between individual **ADI** molecules observed in the pure **ADI** are maintained in the co-crystal structure. All hydrogen bonding details are given in Table 4.25.

Table 4.25. Hydrogen-bond geometry (Å, °) for **13**

X—H····A	X—H	H····A	X····A	∠(XHA)
N8C—H8C····O1B	0.88	2.01	2.884(3)	171
N8B—H8B····O10C[i]	0.88	1.91	2.774(3)	167
O1A—H1A····N1C[ii]	1.05	1.52	2.560(3)	167
O5A—H5A····N1B	1.12	1.52	2.636(3)	175
O8A—H8A····O10B[iii]	0.93	1.66	2.583(3)	170

Symmetry codes: (i) -x-1, -y+1, -z, (ii) x+1, y, z, (iii) x, y-1, z
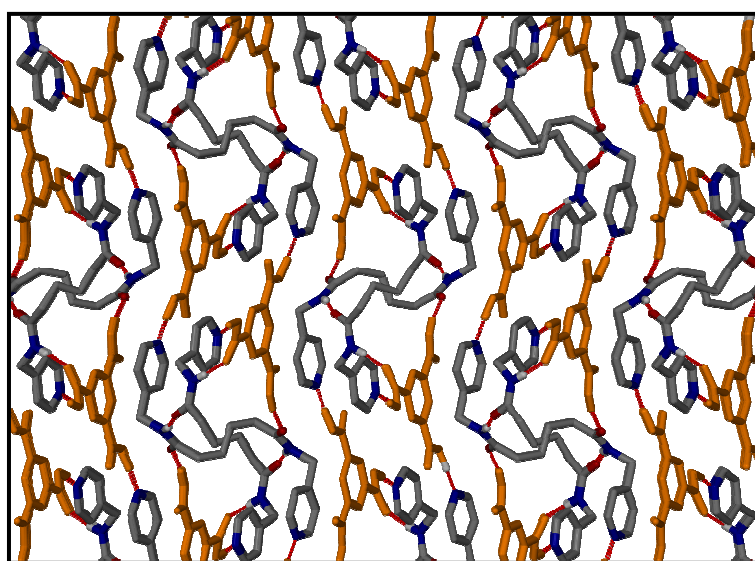

Figure 4.34. Capped stick representation of the packing diagram of **13** viewed along [100]. The trimesic acid molecules have been coloured in light brown and the **ADI** molecules are shown in CPK colours. Hydrogen atoms not involved in hydrogen bonding have been omitted for clarity.
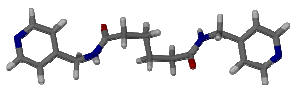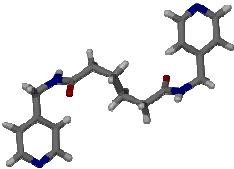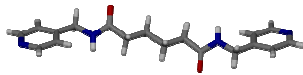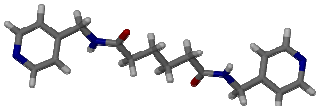
4.2.5   Comparison of complexes 6-12
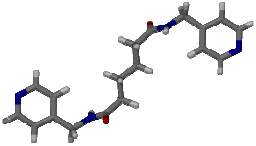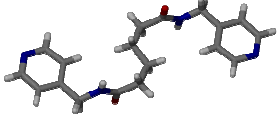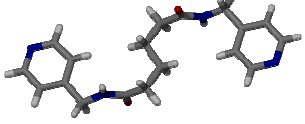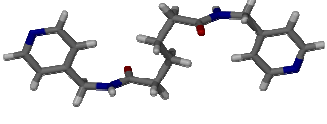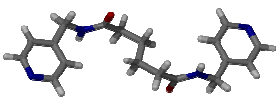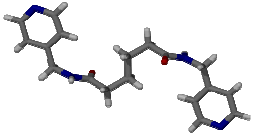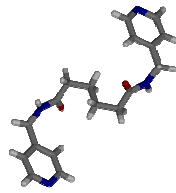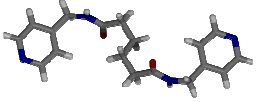
A summary of the comparison between complexes **6-12** is given in Table 4.27.

Conformations of ADI

In the series of ligands synthesized in this study, **ADI** contains the longest spacer group consisting of four sp^3 carbon atoms. The ligand is quite flexible and can adopt a variety of conformations and shapes to meet the geometrical needs of the metal as well as hydrogen bonding needs of the anion and solvent molecules. The ligand conformations and shapes in each complex are shown in Table 4.26. In the present study, it was found that the ligand can be arranged in two conformations, that is the gauche-anti-gauche (GAG) and the anti-anti-anti (AAA). The conformations are given by the sp^3 C−C−C−C torsion angles, G is defined as $180 \geq \theta \geq 90$ and A is defined as $0 \leq \theta \leq 90$.[12,13] The GAG conformation proved to be the common conformation appearing in all complexes except that of **7**.

Table 4.26. Conformations of **ADI**

Compound	Diagram	Torsion angle (º)	Conformation
Pure **ADI**		62.7, -180, 62.7	GAG
6 a		177.8, 180, -177.8	GAG
b		-176.8, 180, -176.8	AAA
c		-179.6, 180, 179	AAA

7		177.8, 180, -177.8	AAA
8		63.9, 180, 63.9	GAG
9		64.5, -180, 64.5	GAG
10		65.5, 180, 65.5	GAG
11		62.7, -180, -62.7	GAG
12		63.9, -180, -63.9	GAG
13 (a)		63.4,180, 63.4	GAG
(b)		67.4, -180, 67.4	GAG

Complex **6** and complex **9** were grown under the same conditions except that the ratio of the metal to ligand was varied.

This resulted in different structures with the ligand adopting the GAG conformation in complex **9** and interestingly, the three independent ligands in complex **6** adopt both AAA and GAG conformations. A similar pattern was noted with complexes **7** and **8**; the complexes were grown from different metal to ligand ratios, and the ligand adopts the AAA conformation in complex **6** and the GAG conformation in complex **8**. It was also noted that in some cases the shape of two ligands may differ even though the conformation is the same. Regardless of the metal salt used, ligands in complexes **8**-**12** prefer to form the GAG conformation.

Self-complementary amide hydrogen bonds

It is interesting to note that of the seven crystal structures of **ADI** obtained in this study, only complex **6** displayed self-complementary amide hydrogen bonds involving **ADI**,[11] and while in the crystal structure of the pure ligand self-complementary amide hydrogen bonds dominate the crystal structure (Section 3.2.3). The amide groups in complexes **8**-**12** are involved in hydrogen bonding interactions between the counter ions as well as the coordinated water molecules and are therefore not available for self-complementary amide hydrogen bonds.

Dimensionality

When considering coordination bonding only, complexes **8**-**12** can be considered to be 1-D chains, complex **6** 2-D, while complex **7** is a 0-D dinuclear complex. However hydrogen bonding interactions between the counter ions, coordinated and uncoordinated water molecules yield a 2-D network in complexes **8**-**12** and a 3-D network in complex **7**. Complex **6** remains 2-D, and hydrogen bonding interactions interlink the 2-D networks.

Table 4.27. Comparison of complexes **8**-**12**

Complex	6	7	8-12
Space group	$P\bar{1}$	$P2_1/c$	$C2/c$
Metal centre coordination geometry	Pentagonal bipyramidal	Distorted octahedral	Distorted octahedral
Dimensionality	2-D	3-D hydrogen bonded network	2-D hydrogen bonded network
Ligand conformation	GAG and AAA	AAA	GAG

4.2.6 Crystal structures obtained with GLUT

This section describes crystal structures obtained from **GLUT** and nitrates of zinc and cadmium. The ligand **GLUT** differs from all the other ligands synthesized in this study in that it contains the 2-aminopyridine moiety instead of the 4-(aminomethyl)pyridine. In both the zinc and the cadmium nitrate complexes the ligand coordinates to the metal centre *via* the pyridyl nitrogen atom and the carbonyl oxygen atom. As a result **GLUT** may be considered to

be a tetradentate chelating ligand, with bite angles of 86.30º for the zinc complex, and 81.13º for the cadmium complex.

4.2.6.1 $\{[Cd(\mathbf{GLUT})(H_2O)_2]\cdot(NO_3)_2\}_n$ **14**
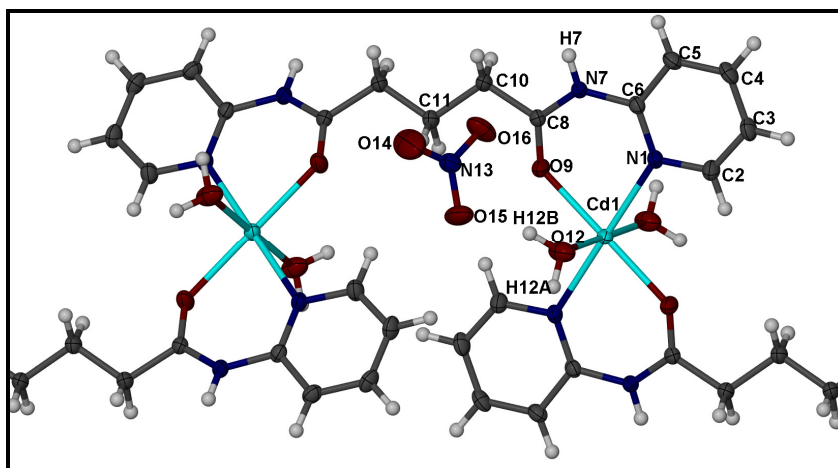
Figure 4.35. The molecular structure of **14** showing the crystallographic labelling scheme and 50% probability ellipsoids for non-hydrogen atoms. Only the asymmetric unit is labelled.

Crystals suitable for SCD analysis were grown by slow evaporation of a solution consisting of **GLUT** and $Cd(NO_3)_2$ in a M:L ratio of 1:4 in ethanol. The complex crystallizes in the monoclinic space group *C*2/*c* with half a Cd(II) cation, one coordinated water molecule, one nitrate anion and half a **GLUT** molecule in the asymmetric unit (Figure 4.35). The cadmium cation, which is coordinated to two **GLUT** ligands *via* two pyridyl nitrogen atoms and two carbonyl oxygen atoms, adopts a distorted octahedral geometry. Coordination geometric parameters are given in Table 4.28. The metal centres are connected by a single **GLUT** molecule to form spiral 1-D chains running along [100] (Figure 4.36).
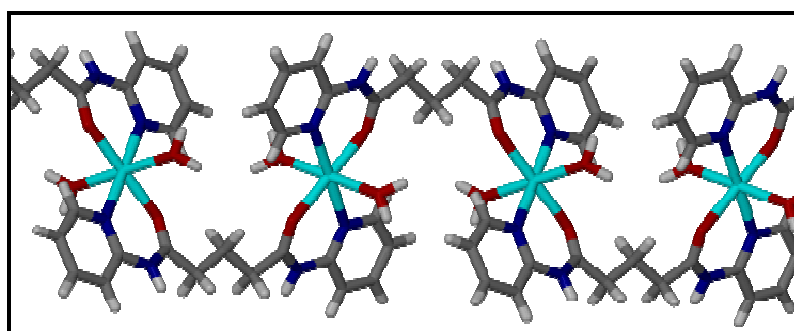
Figure 4.36. Spiral 1-D chains in **14** viewed along [100].

These 1-D chains pack to form two distinct layers which are arranged in an..ABABA… stack. The nitrate anion connects 1-D chains in the same layer by accepting a hydrogen bond from a coordinated water molecule of a chain (O12$-$H12B$\cdots$O14^{ii}) as well as an amide NH of

a parallel chain (N7─H7⸺O16^i) as can be seen in Figure 4.37. The nitrate anion also connects chains in different layers by accepting a hydrogen bond from a coordinated water molecule as well as a hydrogen bond from an amide NH (O12─H12A⸺O16⸺H7─N7) into a 3-D network. The packing diagram is given in Figure 4.38 and all hydrogen bond geometries are given in Table 4.29.
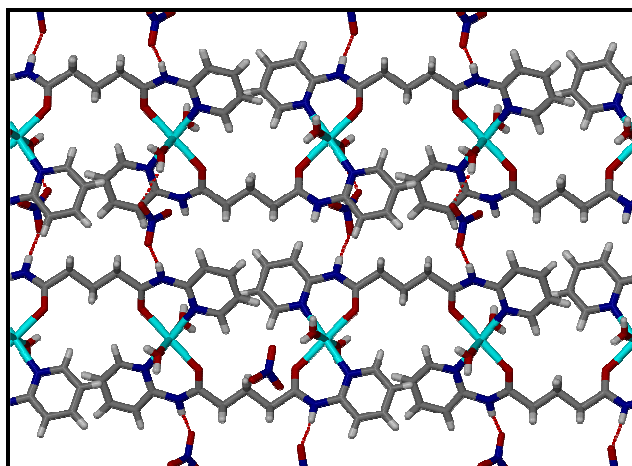
Figure 4.37. The 1-D chains in **14** interact *via* the nitrate anions to form a 2-D layer.

Table 4.28. Coordination geometric parameters (Å, °) for **14**

Distance		Angle	
Cd1─O9^i	2.228(2)	O9^i─Cd1─O9	180.0(6)
Cd1─O9	2.228(2)	O9^i─Cd1─N1	98.8(6)
Cd1─N1	2.282(2)	O9^i─Cd1─N1^i	81.2(6)
Cd1─N1^i	2.282(2)	O9^i─Cd1─O12^i	90.6(1)
Cd1─O12^i	2.330(2)	O9^i─Cd1─O12	89.4(7)
Cd1─O12	2.330(2)	N1^i─Cd1─O12^i	91.9(7)
Angle		N1^i─Cd1─O12	88.1(7)
O9─Cd1─N1	81.2(6)	O12^i─Cd1─O12	180.0(1)
O9─Cd1─N1^i	98.8(6)		
O9─Cd1─O12^i	89.4(7)		
O9─Cd1─O12	90.6(7)		
N1─Cd1─N1^i	180.0		
N1─Cd1─O12^i	88.1(7)		
N1─Cd1─O12	91.9(7)		

Symmetry codes: (i) -x+1/2, y-1/2, -z+1/2

Table 4.29. Hydrogen-bond geometry (Å, °) for **14**

X─H⸺A	X─H	H⸺A	X⸺A	∠(XHA)
N7─H7⸺O15^i	0.88	2.06	2.904(4)	161
O12─H12A⸺O15	0.95	1.89	2.832(4)	166
O12─H12A⸺N13	0.95	2.64	3.563(3)	163
O12─H12B⸺O16^{ii}	0.95	2.13	3.058(4)	164
O12─H12B⸺O14^{ii}	0.95	2.35	3.137(5)	139
O12─H12B⸺N13^{ii}	0.95	2.59	3.523(3)	167

Symmetry codes: (i) -x+1/2, y-1/2, -z+1/2, (ii) -x+1/2, y+1/2, -z+1/2
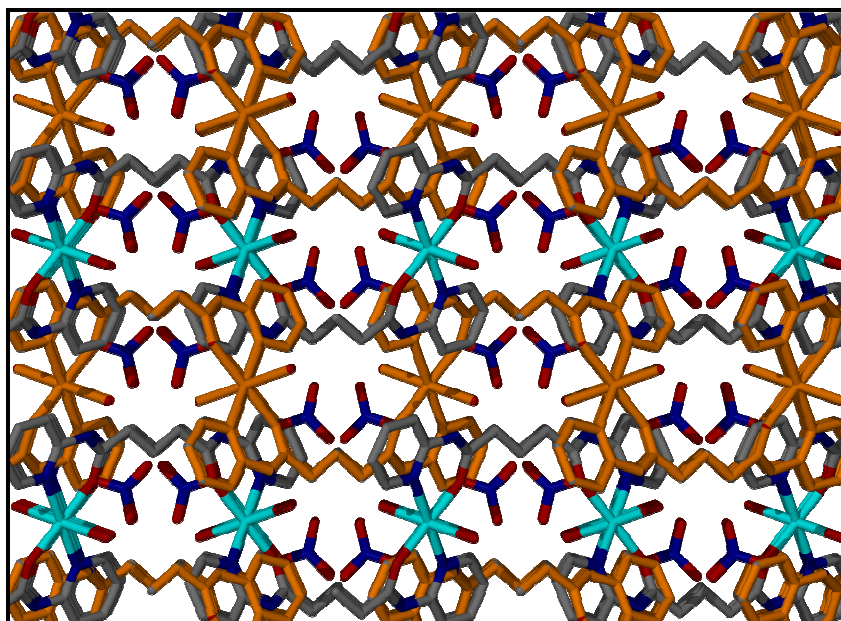
Figure 4.38. The packing diagram of **14**. The chains in the two distinct layers have been coloured in light brown and CPK colours to distinguish them from each other. The hydrogen atoms have been omitted for clarity.

4.2.6.2 $\{[Zn(\textbf{GLUT})(H_2O)_2]\cdot(NO_3)_2\}_n$ **15**

Crystals suitable for SCD analysis were grown from slow evaporation of a solution containing **GLUT** and $Zn(NO_3)_2$ in a metal to ligand ratio of 1:4. The compound crystallizes in the monoclinic space group $C2/c$ with half a zinc cation, half a **GLUT** molecule, one nitrate anion and a coordinated water molecule in the asymmetric unit (Figure4. 39). The metal centre, which is coordinated to two ligands *via* the nitrogen atom and the carbonyl oxygen atoms, adopts a distorted octahedral geometry. Coordination geometric parameters are given in Table 4.30. Complex **15** is isostructural with complex **14** and hence no further crystal descriptions are necessary. The packing diagram of complex **15** is identical to that of complex **14** (Figure 4.38). All hydrogen bonding details are given in Table 4.31.
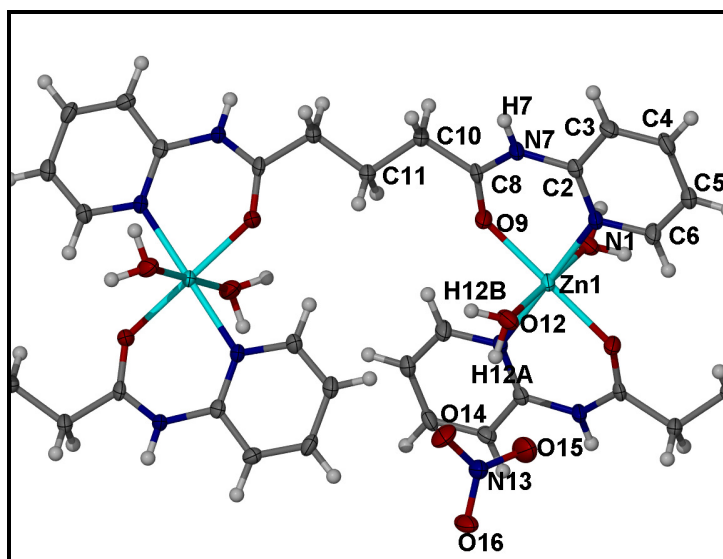
Figure 4.39. The molecular structure of **15** showing atomic labelling scheme and 50% probability ellipsoids for non-hydrogen atoms. Only the asymmetric unit is labelled.

Table 4.30. Coordination geometric parameters (Å, °) for **15**

Distance		Angle	
Zn1−O9	2.052(3)	O9−Zn1−O9^i	180.0
Zn1−O9^i	2.052(3)	O9−Zn1−N1	863(3)
Zn1−N1	2.148(4)	O9−Zn1−N1^i	93.7(2)
Zn1−N1^i	2.148(4)	O9−Zn1−O12^i	88.5(2)
Zn1−O12^i	2.158(4)	O9−Zn1−O12	91.5(2)
Zn1−O12	2.158(4)	N1^i−Zn1−O12^i	90.8(2)
Angle		N1^i−Zn1−O12	89.2(2)
O9^i−Zn1−N1	93.7(2)	O12^i−Zn1−O12	180.0(1)
O9^i−Zn1−N1i	86.3(2)		
O9^i−Zn1−O12^i	91.5(2)		
O9^i−Zn1−O12	88.5(2)		
N1−Zn1−N1^i	180.0		
N1−Zn1−O12^i	89.2(2)		
N1−Zn1−O12	90.8(2)		

Symmetry codes: (i) -x+1/2, -y+3/2, -z

Table 4.31. Hydrogen-bond geometry (Å, °) for **15**

X−H⋯A	X−H	H⋯A	X⋯A	∠(XHA)
N7−H7⋯O16^{ii}	0.88	2.07	2.903(5)	158
O12−H12A⋯O15	0.96	2.10	3.006(5)	158
O12−H12A⋯O14	0.96	2.31	3.079(5)	147
O12−H12A⋯N13	0.96	2.31	3.458(5)	161
O12−H12B⋯O16^{iii}	0.96	2.03	2.844(5)	141

Symmetry codes: (ii) x, y-1, z, (iii) -x+1/2, y-1/2, -z+1/2

4.2.7 Crystal structures obtained with ISO

4.2.7.1 {[Zn(**ISO**)$_2$(H$_2$O)$_2$)]·(NO$_3$)$_4$·(H$_2$O)$_2$}$_n$ 16
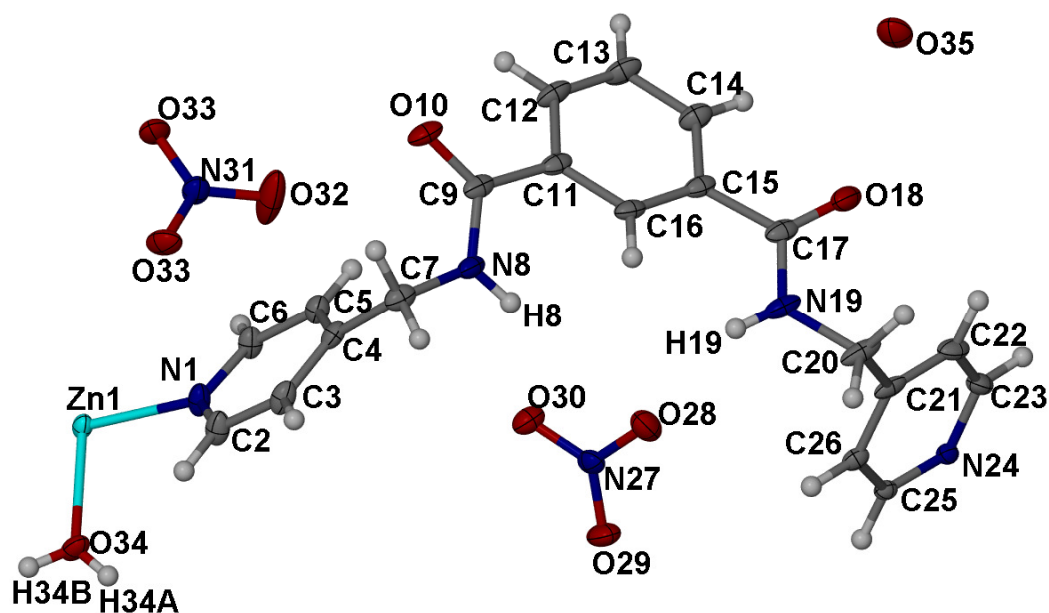
Figure 4.40. The asymmetric unit of **16** showing the crystallographic labelling scheme and 50% probability ellipsoids for non-hydrogen atoms.

Crystals suitable for SCD analysis were obtained by slow evaporation of a water/ethanol solution of zinc nitrate and **ISO** in a 1:1 ratio. The compound crystallizes in monoclinic space group *P2/n*, the asymmetric unit consist of two nitrate anions, a zinc cation with 0.5 occupancy, one **ISO** molecule, one coordinated water molecule and one uncoordinated water molecule. The metal centre is coordinated to four ligands *via* the pyridyl nitrogen atom and also to two water molecules. The coordination geometric parameters are given in Table 4.32. The metal centres are linked by means of two bridging **ISO** ligands to form continuous 1-D looped chains running along [100] (Figure 4.41a). The 1-D chains pack in an offset fashion as can be seen in Figure 4.41b. This offset arrangement is stabilised by three types of hydrogen bonds, in one of these bonds, each coordinated water molecule of a chain donates a hydrogen bond to an amide carbonyl of its two neighbours (O34─H34B⋯O10^v). The remaining hydrogen bonds are facilitated by one of the nitrate anions, with its two oxygen atoms acting as acceptors to two NH groups from the two neighbouring chains (N8─H8⋯O30) and (N19─H19⋯O29^{iv}). The remaining nitrate anion donates a hydrogen bond to one of the coordinated water molecules (O34─H34A⋯O33^v). The hydrogen boding is illustrated in Figure 4.42 and hydrogen bonding details are given in Table 4.33.
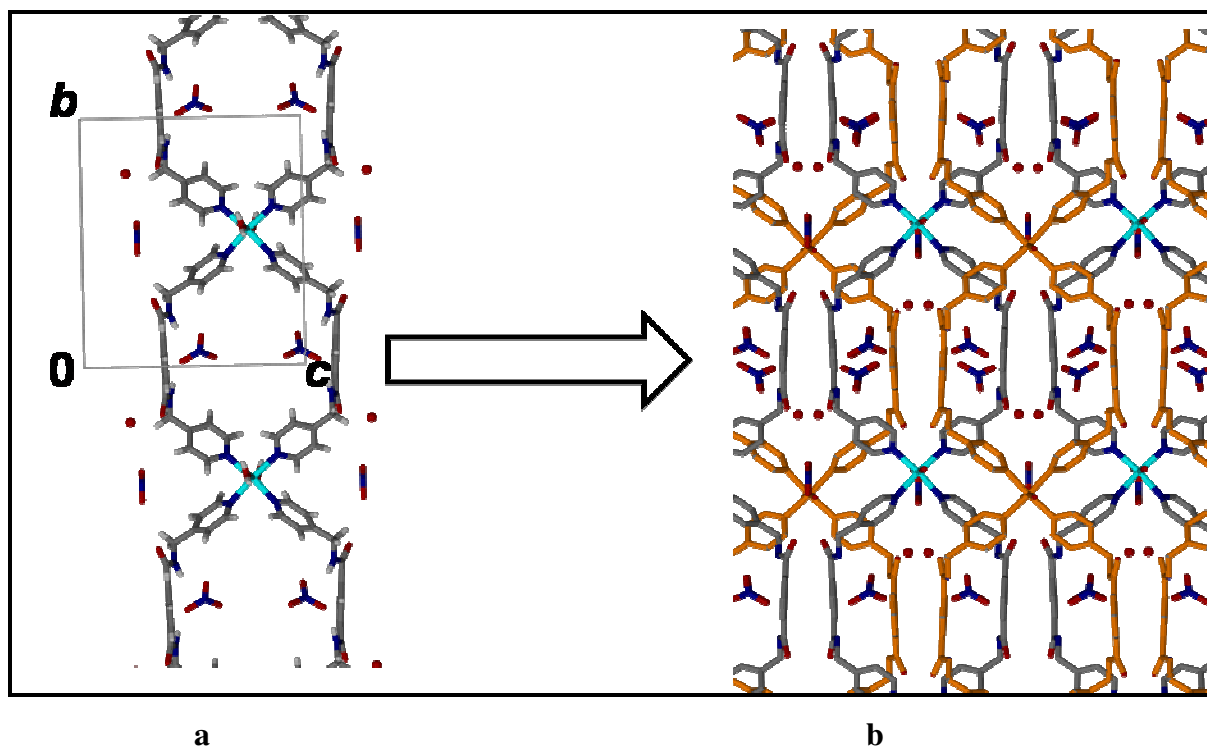
Figure 4.41. (a) 1-D looped chains, (b) the packing diagram of **16** as viewed along [100].

Table 4.32. Coordination geometric parameters (Å, º) for **16**

Distance		Angle	
Zn1—N1	2.132(2)	N1—Zn1—N1^{i}	86.4(8)
Zn1—N1^{i}	2.132(2)	N1—Zn1—N1^{ii}	173.1(6)
Zn1—N24^{ii}	2.141(1)	N1—Zn1—N24^{iii}	89.0(6)
Zn1—N24^{iii}	2.141(1)	N1—Zn1—O34	91.9(6)
Zn1—O34	2.191(1)	N1—Zn1—O34i	95.1(6)
Zn1—O34^{i}	2.199(1)	N24^{iii}—Zn1—O34	90.1(5)
Angle		N24^{iii}—Zn1—O34^{i}	83.5(6)
N1^{i}—Zn1—N24^{ii}	89.0(7)	O34—Zn1—O34^{i}	170.5(8)
N1^{i}—Zn1—N24^{iii}	173.1(6)		
N1^{i}—Zn1—O34	95.1(6)		
N1^{i}—Zn1—O34^{i}	91.9(6)		
N24^{ii}—Zn1—N24^{ii}	96.1(7)		
N24^{ii}—Zn1—O34	83.5(6)		
N24^{ii}—Zn1—O34^{i}	90.1(5)		

Symmetry codes: (i) -*x*+3/2, *y*, -*z*+3/2, (ii) -*x*+3/2, *y*+1, -*z*+3/2, (iii) *x*, *y*+1, *z*

Table 4.33. Hydrogen-bond geometry (Å, °) for **16**

X－H⋯A	X－H	H⋯A	X⋯A	∠(XHA)
N19－H19⋯O29^{iv}	0.88	2.13	2.821(3)	134
N19－H19⋯O28	0.88	2.26	3.095(3)	159
N8－H8⋯O30	0.88	2.08	2.829(2)	142
O34－H34B⋯O10^{v}	0.96	1.95	2.895(2)	169
O34－H34A⋯O33^{v}	0.96	1.91	2.849(2)	166
O34－H34A⋯O32^{vi}	0.96	2.29	3.022(1)	132
O34－H34A⋯N31^{vi}	0.96	2.43	3.356(2)	162

Symmetry codes: (iv) $-x+2$, $-y$, $-z+1$, (v) $x+1/2$, $-y+1$, $z+1/2$, (vi) $-x+2$, $-y+1$, $-z+1$
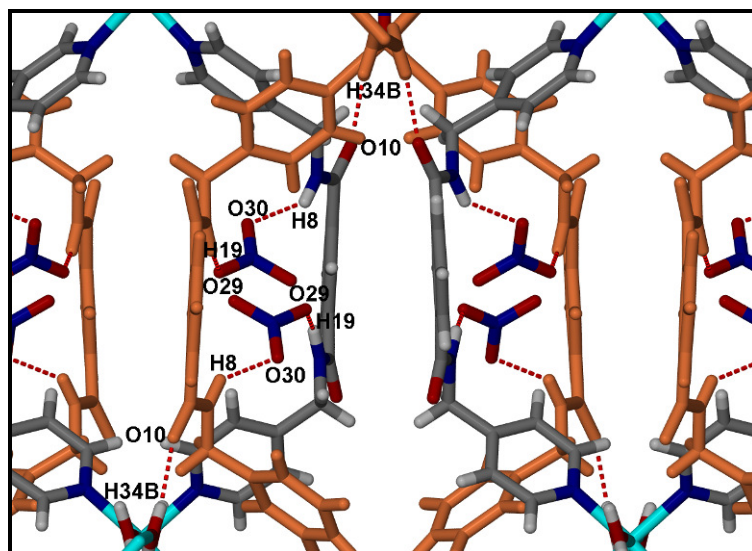
Figure 4.42. An expanded view of the hydrogen bond interactions between 1-D chains in **16**.

4.2.8 Crystal structures obtained with TER-A

4.2.8.1 {[Zn(**TER-A**)$_2$(H$_2$O)]·(H$_2$O)$_3$·(DMF)}$_n$ **17**

Crystals suitable for SCD analysis were gown by slow evaporation of a DMF solution of **TER-A** and Zn(NO$_3$)$_2$ in a M:L ratio of 1:2. The complex crystallizes in the triclinic space group $P\bar{1}$ with a zinc cation, two **TER-A** molecules, one DMF molecule and three coordinated water molecules in the asymmetric unit (Figure 4.43). The metal centre which adopts a pentagonal bipyramidal geometry is coordinated to two ligands *via* two pyridyl nitrogen atoms and two ligands *via* four carboxylic acid oxygen atoms, the oxygen atoms coordinate in a chelating fashion. The coordination geometric parameters are given in Table 4.34.
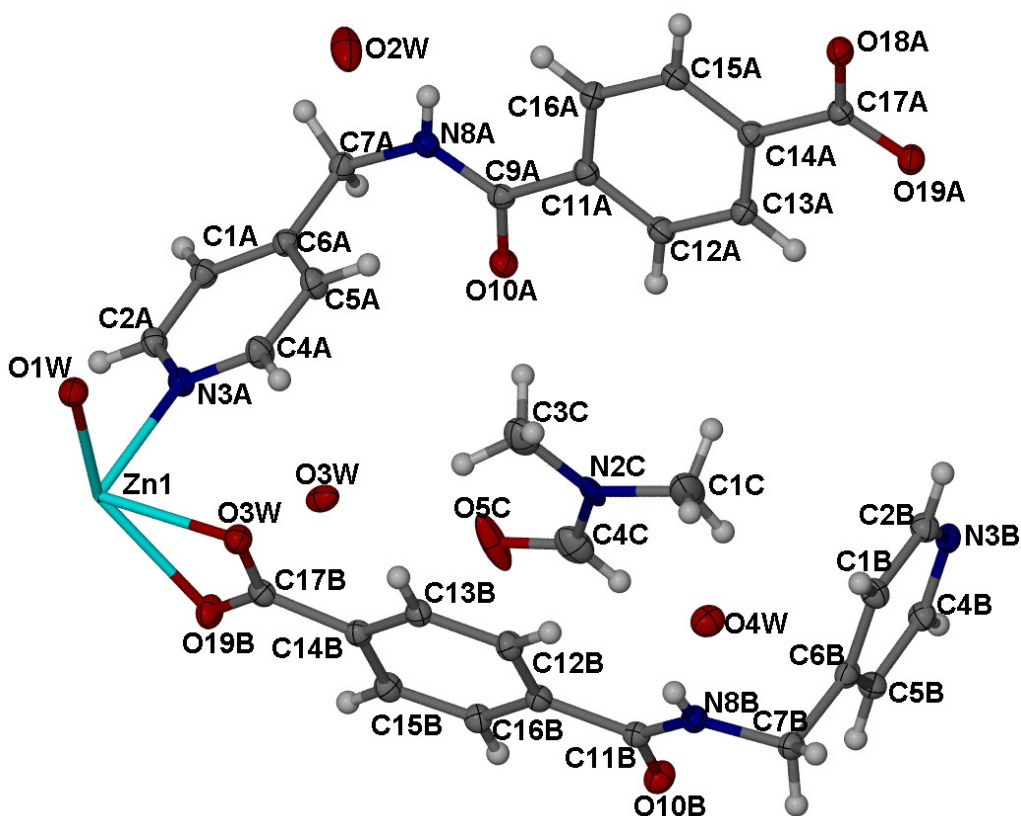
Figure 4.43. The asymmetric unit of **17** showing ellipsoids at 30% probabilty level and the atomic labelling scheme used.

The metal centres are linked by bridging **TER-A** ligands to form polymeric 2-D networks which form channels along the crystallographic *a* axis, the channels are occupied by DMF molecules (Figures 4.44 and 4.45).
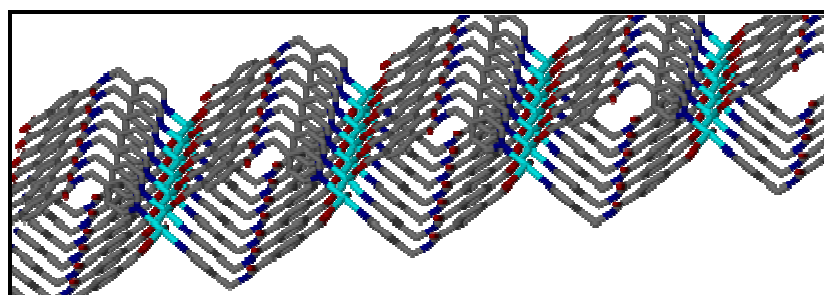
Figure 4.44. The metal centres are linked by ligand molecules to form a 2-D network which has channels along the *a* axis. The water molecules, DMF molecule and the hydrogen atoms have been omitted for clarity.
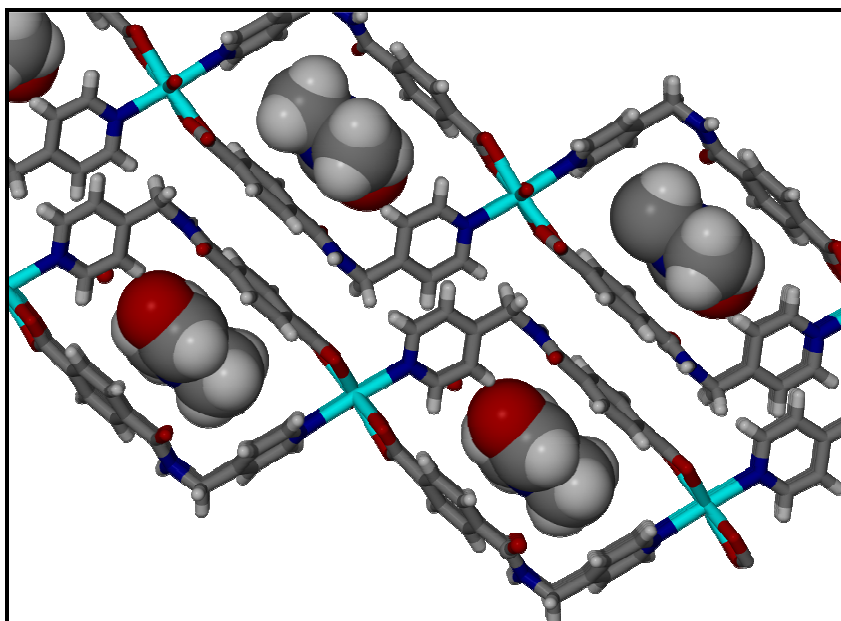
Figure 4.45. The packing diagram of **17** viewed along [100]. The ligand molecules are shown in capped stick format while the DMF is shown with van der Waals radii**.**

Table 4.34. Coordination geometric parameters (Å, º) for **17**

Distance		Angle	
Zn1$-$N3A	2.291(5)	N3A$-$Zn1$-$N3B^i	176.2(2)
Zn1$-$N3B^i	2.359(5)	N3A$-$Zn1$-$O18A^{ii}	97.3(2)
Zn1$-$O18A^{ii}	2.375(4)	N3A$-$Zn1$-$O1W	89.1(2)
Zn1$-$O1W	2.393(4)	N3A$-$Zn1$-$O19A^{ii}	97.7(2)
Zn1$-$19A^{ii}	2.405(5)	N3A$-$Zn1$-$O19B	90.1(2)
Zn1$-$O19B	2.439(5)	N3A$-$Zn1$-$O18B	88.4(2)
Zn1$-$O18B	2.445(4)	O18A^{ii}$-$Zn1$-$O1W	86.5(2)
Angle		O18A^{ii}$-$Zn1$-$O19^{ii}	55.12(2)
N3B^i$-$Zn1$-$O18A^{ii}	85.2(2)	O18A^{ii}$-$Zn1$-$O19B	134.6(2)
N3B^i$-$Zn1$-$O1W	88.4(2)	O18A^{ii}$-$Zn1$-$O18B	169.4(2)
N3B^i$-$Zn1$-$O19A	85.9(2)	O19A^{ii}$-$Zn1$-$O19B	79.5(2)
N3B^i$-$Zn1$-$O19B	89.5(2)	O19A^{ii}$-$Zn1$-$O18B	133.2(2)
N3B^i$-$Zn1$-$O18B	88.7(2)	O19B$-$Zn1$-$O18B	53.9(1)
O1W$-$Zn1$-$O19A^{ii}	141.5(2)		
O1W$-$Zn1$-$O19B	138.4(2)		
O1W$-$Zn1$-$O18B	84.6(2)		

Symmetry codes: (i) *x*, *y*-1, *z* (ii) *x*+1, *y*-1, *z*

4.3   General discussion

Crystal structures of sixteen novel coordination complexes and one novel co-crystal are described here. In complexes **1**-**5**, generally, the structures consist of 1-D polymeric chains in which a single ligand bridges the metal centres. The metal centres in complexes **2**-**5** adopt distorted octahedral geometry while, in complex **1**, the metal centre is in a distorted trigonal bipyramidal arrangement. Water molecules are included in all the crystal structures (both coordinated and uncoordinated) and hydrogen bonding between these and the counter ions as well as the amide groups link the 1-D chains into higher dimensions. Regarding the role played

by the metal counterion on the nature of the final assembly, it is clear from the structures of complexes **1** and **2** that the nature of metal counterions can greatly influence the final structure. This may be attributed to their different sizes, geometry and their hydrogen bonding interactions between the ligand and the solvent molecules.

In complexes **6**-**12** the ligand adopts two conformations: GAG and AAA. Two different structures were obtained with $Zn(NO_3)_2$ by varying the M:L ratio. In both complexes, the Zn(II) centre adopts octahedral geometry, the counter ion is non coordinating and involved in hydrogen bonding interactions between water molecules and the amide group. The two structures differ in two ways. First, complex **7** is discrete and dinuclear, while complex **8** forms continuous 1-D chains. Second, the ligand in complex **7** adopts AAA conformation while in complex **9** the ligand adopts GAG conformation. The same comparison can be made between complexes **6** and **9**, which were grown from $Cd(NO_3)_2$ by varying the M:L ratio. The two complexes differ in the following ways:

- The anion in complex **6** coordinates to the metal centre, while in complex **9** the anion is non coordinating;

- Complex **6** is a 2-D brick-like layer while complex **9** is a 1-D continuous chain;

- In complex **9** the Cd(II) centre adopts octahedral geometry while in complex **6** the Cd(II) is pentagonal bipyramidal;

- The ligands in complex **6** adopt both GAG and AAA conformations while in complex **9** only the GAG conformation is observed;

- In complex **6** one of the amide carbonyl oxygen atoms coordinates to the metal centre while in complex **9** the amide carbonyl is noncoordinating;

- One set of self-complementary amide hydrogen bonds is observed in complex **6**, while in complex **9** all the amide groups are involved in hydrogen bonding between the anions and the water molecules.

Complexes **8**-**12** are isostructural, even though the metal centres and the counterions are different. The bromide, chloride and the nitrate anions assume the same role in all complexes and the ligand adopts the GAG conformation. Compound **13** is a 1:1 co-crystal of trimesic acid and **ADI**. The two molecules interact *via* the utilization of the pyridine/carboxylic acid and the amide/carboxylic acid heterosynthons, while **ADI** molecules interact with each other *via* the amide homosynthon. Complexes **14** and **15** are isostructural; the ligand binds to the metal centre in a tetradentate mode and no water molecules are included in the structure. It would be interesting to determine whether the tetradentate mode persists even when the ligand is crystallized with silver salts. Complex **16** consists of looped 1-D chains. Adding a second ligand such as 2,2'-bipyridine would be interesting since there is a possibility of forming a

discrete zero dimensional complex provided the 2,2'-bipyridine chelates to the metal centre.[14] In complex **17** DMF molecules have been included in the structures and these are located in channels. The crystal structure is free of counterions owing to the charge balancing effect of the anionic carboxylate functional group. Due to the low yield of the product, it was not possible to carry out any thermogravimetric analysis to determine whether the framework can survive the process of guest removal.

4.4 References

1. R. Villar, P. Diaz, and A. J. P. White, *Inorg. Chem.*, 2006, **45**, 1617.

2. S. L. James, *Chem. Soc. Rev*, 2003, **32**, 276.

3. T. A. Okamura, G. C. Xu, Y. Q. Huang, G. X. Liu, W. Y. Sun and N. Ueyama, *CrystEngComm*, 2008, **10**, 1052.

4. M. W. Hosseini, *CrystEngComm*, 2004, **6**, 318.

5. S. Muthu, J. H. K. Yip and J. J. Vittal, *J. Chem., Dalton Trans.,* 2002, 4561.

6. H. Matsuzaka and Y. Yamashita, *J. Am. Chem., Soc,* 2002, **124**, 2568.

7. O-S. Jung, Y. J. Kim, Y. A. Lee, J. K. Park and H. K. Chae, *J. Am. Chem. Soc.*, 2000, **122**, 9921.

8. B-C. Tzeng, Y-C. Huang, B-S. Chem, W-M. Wu, S-Y Lee, G-H. Lee and S-H. Peng, *Inorg. Chem.*, 2007, **46**, 186.

9. H. Hu, Y. Hsu, C. Wu, C. Yeh, D. M. Proserpio and J. Chen, *CrystEngComm,*, 2009, **11**, 168.

10. G. O. Lloyd, *Acta Cryst. Sect. E,* 2005, **E61**, o1218.

11. R. Taylor and O. Kennard, *Acc. Chem. Res*, 1984, **17**, 320.

12. K. Atticks; R. K. Bohn; H. H. Michels, *Int. J. Quantum. Chem.* 2001, **85**, 514.

13. H.-C. Chen, H-L. Hu, Z-K Chan, C-W. Yeh, H-W Jia, C-P. Wu, J-D. Chen, and J-C. Wang, *Cryst.Growth Des.,* 2007, **7**, 69.

14. M. J. Plater, S. Buchan, M. R. Foreman, B. M. De Silva, M. Z. Alexander and J. M. Slawin, *J. Chem. Cryst.* 2002, **32**, 5.

Table 4.35. The crystallographic data of **1-5**

	1	2	3	4	5
Empirical formula	$C_{16}H_{22}CuN_4O_{11}S$	$C_8H_{12}Cu_{0.50}N_3O_7$	$C_8H_{14}ClN_2Ni_{0.50}O_4$	$C_{16}H_{28}Cl_2CoN_4O_8$	$C_8H_{15}ClCo_{0.50}N_2O_4$
Formula weight	541.98	293.98	267.02	267.13	268.14
Temperature (K)	173(2)	173(2)	173(2)	173(2)	173(2)
Wavelength (Å)	0.71073	0.71073	0.71073	0.71073	0.71073
Crystal system	monoclinic	monoclinic	monoclinic	monoclinic	monoclinic
a/ Å	9.0463(10)	10.6368(14)	8.864(2)	8.756(7)	8.7563(7)
b/ Å	15.1802(17)	13.7609(17)	14.986(3)	15.049(2)	15.247(1)
c/ Å	15.9831(18)	8.4977(11)	8.85562)	8.876(2)	8.9545(7)
β/°	3.873(2)	104.421(2)	96.909(2)	96.705(2)	96.519(1)
Space group	$P2_1/c$	$P2_1/c$	$P2_1/c$	$P2_1/c$	$P2_1/c$
Volume (Å^3)	2189.9(4)	1204.6(3)	1167.8(4)	1178.2(3)	1187.73(2)
Z	4	4	4	4	4
Calculated density (g cm^{-3})	1.644	1.621	1.519	1.506	1.499
Absorption coefficient (mm^{-1})	1.159	0.988	1.107	1.003	0.995
F_{000}	1116	606	556	554	558
Crystal size (mm^3)	$0.19 \times 0.18 \times 0.18$	$0.30 \times 0.24 \times 0.16$	$0.40 \times 0.40 \times 0.20$	$0.33 \times 0.25 \times 0.19$	$0.39 \times 0.22 \times 0.18$
θ range for data collection (°)	1.85 to 28.24	1.98 to 27.97	2.31 to 25.51	2.31 to 25.52	2.34 to 26.71
Miller index ranges	$-11 \leq h \leq 11$, $-13 \leq k \leq 19$, $-20 \leq l \leq 18$	$-13 \leq h \leq 9$, $-17 \leq k \leq 16$, $-11 \leq l \leq 9$	$-10 \leq h \leq 10$, $-15 \leq k \leq 18$, $-9 \leq l \leq 10$	$-10 \leq h \leq 10$, $-18 \leq k \leq 17$, $-5 \leq l \leq 10$	$-11 \leq h \leq 11$, $-17 \leq k \leq 18$, $-11 \leq l \leq 7$
Reflections collected	13604	7126	6218	6317	6886
Independent reflections	5074 [$R_{int} = 0.0279$]	2627 [$R_{int} = 0.0237$]	2161 [$R_{int} = 0.0275$]	2190 [$R_{int} = 0.0301$]	2452 [$R_{int} = 0.0294$]
Completeness to θ_{max} (%)	93.7	90.8	99.4	99.5	97.2
Max. and min. transmission	0.8185 and 0.8098	0.8579 and 0.7559	0.8089 and 0.6657	0.8324 and 0.7332	0.8413 and 0.6977
Refinement method	Full-matrix least-squares on F^2	Full-matrix least-squares on F^2	Full-matrix least-squares on F^2	Full-matrix least-squares on F^2	Full-matrix least-squares on F^2
Data / restraints / parameters	5074 / 0 / 322	2627 / 0 / 185	2161 / 0 / 161	2190 / 0 / 157	2452 / 0 / 157
Goodness-of-fit on F^2	1.035	1.105	1.098	1.060	1.020
Final R indices [$I > 2\sigma(I)$]	$R1 = 0.0357$, $wR2 = 0.0950$	$R1 = 0.0484$, $wR2 = 0.1322$	$R1 = 0.0368$, $wR2 = 0.0833$	$R1 = 0.0388$, $wR2 = 0.0905$	$R1 = 0.0334$, $wR2 = 0.0775$
R indices (all data)	$R1 = 0.0397$, $wR2 = 0.0978$	$R1 = 0.0484$, $wR2 = 0.1322$	$R1 = 0.0368$, $wR2 = 0.0833$	$R1 = 0.0388$, $wR2 = 0.0905$	$R1 = 0.0426$, $wR2 = 0.0830$
Largest diff. peak and hole (e Å^{-3})	0.716 and -0.608	0.568 and -1.460	0.472 and -0.296	0.421 and -0.365	0.575 and -0.535

Table 4.36. The crystallographic data of **6-10**

	6	7	8	9	10
Empirical formula	$C_{27}H_{33}CdN_8O_9$	$C_9H_{23}N_4O_{13}Zn$	$C_{18}H_{34}N_6O_{14}Zn$	$C_{18}H_{34}CdN_6O_{14}$	$C_{18}H_{34}CuN_6O_{14}$
Formula weight	726.01	460.68	623.88	670.91	622.05
Temperature (K)	173(2)	173(2)	173(2)	173(2)	173(2)
Wavelength (Å)	0.71073	0.71073	0.71073	0.71073	0.71073
Crystal system	triclinic	monoclinic	monoclinic	monoclinic	monoclinic
a/ Å	9.764(2)	14.1385(3)	23.217(2)	23.6478(18)	22.699(6)
b/ Å	11.995(2)	11.7744(3)	8.2036(8)	8.3421(6)	8.248(2)
c/ Å	14.154(3)	11.3347(3)	16.0028(16)	15.9843(12)	16.097(4)
α/°	82.23(3)				
β/°	77.44(3)	99.1890(10)	115.8530(10)	117.0740(10)	115.124(3)
γ/°	69.54(3)				
Space group	$P\bar{1}$	$P2_1/c$	$C2/c$	$C2/c$	$C2/c$
Volume (Å^3)	1512.9(5)	1862.70(8)	2742.9(5)	2807.7(4)	2728.8(12)
Z	2	4	4	4	4
Calculated density (g cm^{-3})	1.594	1.643	1.511	1.587	1.514
Absorption coefficient (mm^{-1})	0.788	1.391	0.971	0.852	0.877
F_{000}	742	956	1304	1376	1300
Crystal size (mm^3)	$0.39 \times 0.35 \times 0.21$	$0.55 \times 0.29 \times 0.13$	$0.40 \times 0.34 \times 0.22$	$0.25 \times 0.20 \times 0.10$	$0.30 \times 0.19 \times 0.17$
θ range for data collection (°)	1.48 to 27.15	2.26 to 28.36	1.95 to 27.88	1.93 to 27.94	1.98 to 27.87
Miller index ranges	$-12 \leq h \leq 11$, $-15 \leq k \leq 15$, $-15 \leq l \leq 18$	$-18 \leq h \leq 15$, $-15 \leq k \leq 15$, $-15 \leq l \leq 15$	$-28 \leq h \leq 28$, $-10 \leq k \leq 10$, $-19 \leq l \leq 19$	$-29 \leq h \leq 28$, $-7 \leq k \leq 10$, $-17 \leq l \leq 19$	$-29 \leq h \leq 29$, $-8 \leq k \leq 10$, $-21 \leq l \leq 11$
Reflections collected	9115	23976	14789	8199	7859
Independent reflections	6297 [R_{int} = 0.0118]	4649 [R_{int} = 0.0386]	3077 [R_{int} = 0.0223]	3092 [R_{int} = 0.0224]	2988 [R_{int} = 0.0535]
Completeness to θ_{max} (%)	93.8	99.7	93.7	91.7	92.1
Max. and min. transmission	0.8520 and 0.7486	0.8398 and 0.5150	0.8147 and 0.6973	0.9196 and 0.8152	0.8653 and 0.7789
Refinement method	Full-matrix least-squares on F^2	Full-matrix least-squares on F^2	Full-matrix least-squares on F^2	Full-matrix least-squares on F^2	Full-matrix least-squares on F^2
Data / restraints / parameters	6297 / 0 / 407	4649 / 0 / 292	3077 / 0 / 201	3092 / 0 / 201	2988 / 0 / 201
Goodness-of-fit on F^2	1.049	1.016	1.026	1.058	1.002
Final R indices [$I > 2\sigma(I)$]	$R1$ = 0.0250, $wR2$ = 0.0687	$R1$ = 0.0290, $wR2$ = 0.0743	$R1$ = 0.0239, $wR2$ = 0.0668	$R1$ = 0.0227, $wR2$ = 0.0518	$R1$ = 0.0497, $wR2$ = 0.1130
R indices (all data)	$R1$ = 0.0277, $wR2$ = 0.0699	$R1$ = 0.0396, $wR2$ = 0.0784	$R1$ = 0.0263, $wR2$ = 0.0685	$R1$ = 0.0227, $wR2$ = 0.0518	$R1$ = 0.0842, $wR2$ = 0.1303
Largest diff. peak and hole (e Å^{-3})	0.807 and -0.680	0.798 and -0.369	0.496 and -0.240	0.660 and -0.261	0.633 and -0.542

Table 4.37. The crystallographic data of **11-15**

	11	12	13	14	15
Empirical formula	$C_{36}H_{68}Cl_4Co_2N_8O_{16}$	$C_9H_{11}BrMn_{0.50}N_2O_4$	$C_{27}H_{28}N_4O_8$	$C_{60}H_{80}Cd_4N_{24}O_{40}$	$C_{7.50}H_{10}N_3O_5Zn_{0.50}$
Formula weight	1128.64	318.58	536.53	2227.08	254.87
Temperature (K)	173(2)	173(2)	173(2)	173(2)	173(2)
Wavelength (Å)	0.71073	0.71073	0.71073	0.71073	0.71073
Crystal system	monoclinic	monoclinic	monoclinic	monoclinic	monoclinic
a/ Å	22.949(6)	22.920(4)	9.1417(2)	14.5031(8)	14.380(15)
b/ Å	7.6484(18)	7.8045(14)	16.1206(4)	10.5730(6)	10.311(10)
c/ Å	17.186(4)	17.297(3)	17.2441(4)	15.8307(9)	15.545(16)
β/°	119.148(3)	116.966(2)	101.045(2)	114.8430(10)	113.634(12)
Space group	$C2/c$	$C2/c$	$P2_1/n$	$C2/c$	$C2/c$
Volume ($Å^3$)	2634.5(11)	2757.6(9)	2494.19(10)	2202.9(2)	2112(4)
Z	2	8	4	1	8
Calculated density (g cm^{-3})	1.423	1.535	1.429	1.679	1.603
Absorption coefficient (mm^{-1})	0.901	3.420	0.107	1.055	1.229
F_{000}	1180	1268	1128	1120	1048
Crystal size (mm^3)	$0.31 \times 0.23 \times 0.13$	$0.40 \times 0.34 \times 0.29$	$0.40 \times 0.25 \times 0.22$	$0.35 \times 0.22 \times 0.18$	$0.40 \times 0.33 \times 0.22$
θ range for data collection (°)	2.03 to 27.78	2.49 to 28.05	1.74 to 28.31	2.47 to 27.69	2.51 to 27.96
Miller index ranges	$-17 \leq h \leq 29$, $-9 \leq k \leq 9$, $-22 \leq l \leq 20$	$-23 \leq h \leq 29$, $-10 \leq k \leq 8$, $-22 \leq l \leq 21$	$-12 \leq h \leq 12$, $-18 \leq k \leq 21$, $-18 \leq l \leq 22$	$18 \leq h \leq 12$, $-13 \leq k \leq 13$, $-14 \leq l \leq 20$	$15 \leq h \leq 18$, $-9 \leq k \leq 13$, $-19 \leq l \leq 19$
Reflections collected	7361	8070	23628	6385	5578
Independent reflections	2804 [$R_{int} = 0.0629$]	3016 [$R_{int} = 0.0290$]	6133 [$R_{int} = 0.0990$]	2391 [$R_{int} = 0.0127$]	2203 [$R_{int} = 0.0667$]
Completeness to $θ_{max}$ (%)	90.3	90.2	98.8	92.7	86.5
Max. and min. transmission	0.8919 and 0.7676	0.4371 and 0.3416	0.9769 and 0.9585		0.7738 and 0.6392
Refinement method	Full-matrix least-squares on F^2	Full-matrix least-squares on F^2	Full-matrix least-squares on F^2	Full-matrix least-squares on F^2	Full-matrix least-squares on F^2
Data / restraints / parameters	2804 / 6 / 174	3016 / 0 / 150	6133 / 0 / 355	0.8329 and 0.7091	2203 / 0 / 155
Goodness-of-fit on F^2	1.009	1.054	0.972	1.059	1.017
Final R indices [$I > 2σ(I)$]	$R1 = 0.0529$, $wR2 = 0.1005$	$R1 = 0.0559$, $wR2 = 0.1552$	$R1 = 0.0622$, $wR2 = 0.1047$	$R1 = 0.0240$, $wR2 = 0.0686$	$R1 = 0.0544$, $wR2 = 0.1378$
R indices (all data)	$R1 = 0.0972$, $wR2 = 0.1164$	$R1 = 0.0960$, $wR2 = 0.1778$	$R1 = 0.0622$, $wR2 = 0.1047$	$R1 = 0.0279$, $wR2 = 0.0724$	$R1 = 0.0819$, $wR2 = 0.1593$
Largest diff. peak and hole (e Å^{-3})	0.448 and -0.797	0.880 and -0.732	0.345 and -0.318	0.467 and -0.277	0.820 and -1.008

Table 4.38. The crystallographic data of **16** and **17**

	16	17
Empirical formula	$C_{20}H_{20}N_5O_{7.50}Zn_{0.50}$	$C_{15.01}H_{13.36}N_{2.34}O_{4.98}Zn_{0.50}$
Formula weight	483.10	338.88
Temperature (K)	173(2)	173(2)
Wavelength (Å)	0.71073	0.71073
Crystal system	monoclinic	triclinic
a/Å	10.2983(9)	6.4817(8)
b/ Å	15.4470(13)	13.7460(17)
c/ Å	13.7562(12)	19.262(2)
α/°		71.6000(10)
β/°	90.690(2)	83.6540(10)
γ/°		81.3210(10)
Space group	$P2/n$	$P\bar{1}$
Volume (Å^3)	2188.1(3)	1606.2(3)
Z	4	4
Calculated density (g cm^{-3})	1.466	1.401
Absorption coefficient (mm^{-1})	0.642	0.826
F_{000}	1000	699
Crystal size (mm^3)	$0.28 \times 0.20 \times 0.18$	$0.50 \times 0.30 \times 0.20$
θ range for data collection (°)	1.32 to 28.05	1.12 to 28.05
Miller index ranges	$-13 \leq h \leq 13$, $-20 \leq k \leq 20$, $-18 \leq l \leq 18$	$-8 \leq h \leq 8$, $-18 \leq k \leq 17$, $-23 \leq l \leq 24$
Reflections collected	24092	18092
Independent reflections	5017 [$R_{int} = 0.0321$]	6999 [$R_{int} = 0.0274$]
Completeness to θ_{max} (%)	94.1	89.7
Max. and min. transmission	0.8931 and 0.8406	0.8521 and 0.6827
Refinement method	Full-matrix least-squares on F^2	Full-matrix least-squares on F^2
Data / restraints / parameters	5017 / 0 / 321	6999 / 2 / 438
Goodness-of-fit on F^2	1.075	1.070
Final R indices [$I > 2\sigma(I)$]	$R1 = 0.0382$, $wR2 = 0.1007$	$R1 = 0.0691$, $wR2 = 0.2156$
R indices (all data)	$R1 = 0.0435$, $wR2 = 0.1041$	$R1 = 0.0756$, $wR2 = 0.2231$
Largest diff. peak and hole (e Å^{-3})	0.680 and -0.227	2.526 and -0.712

Chapter 5

Conclusion

5.1   Concluding remarks

Eight structurally related bis-pyridyl diamide ligands were synthesized and characterized as described in Chapter 2. In Chapter 3, the crystal structures of **TER**, **ADI**, **DIP**, **GLUT** and **TER-A** were described. Of these, only the crystal structures of **ADI** and **TER-A** featured the self-complementary amide hydrogen bonds while in the remaining crystal structures, the amide group is hydrogen bonded to the water molecules.

In Chapter 4, seventeen novel crystal structures were described: four containing **FUM**, one containing **SUC,** eight containing **ADI,** two containing **GLUT,** one containing **ISO** and one containing **TER-A**. Even though the motivation behind this work was to make crystals with interesting structural features, such as helical structures,[1] water clusters[2] and porosity[3], none of the seventeen crystal structures reported in this work possess any of the above mentioned properties. Nonetheless, we were able to study by SCD analysis the self assembly processes of the seventeen crystal structures.

Each crystal structure was described in terms of the nature of the building blocks, the type of intermolecular interactions, the geometry of the metal centre and the dimensionality of the network.[4] Similarities and differences between the packing motifs of structures containing the same ligand were also highlighted. In one instance, it was possible to determine the role played by the nature of the counterion in the final assembly (complex **1** and **2**) and in two instances we were able to study the effect of varying the M:L ratio on the nature of the final assembly (**6** and **9**) and (**7** and **8**).

Since the amide group has been shown to assemble *via* self-complementary amide hydrogen bonds, we expected the amide groups to interact with one another *via* such known patterns of self assembly.[5] However, in fifteen of the seventeen crystal structures described in Chapter 4, the amide bond is hydrogen bonded to either water molecules or metal counterions. In the remaining two structures, only one amide group is involved in self-complementary amide hydrogen bonding and the values are within the range of other reported distances[5] (for **6** N8$-$H8$\cdots$O22 = 2.788(3) Å) and (for **13** N8B$-$H8B$\cdots$O10C = 2.774(3) Å). Several examples have also been reported where the amide group has participated in hydrogen bonding interactions with other molecular species instead of interacting *via* the amide homosynthon.[6,7]

The distorted octahedral coordination geometry proved to be the most common metal coordination geometry, occurring in metal centres of all complexes except in three complexes.

In complexes **6** and **17** the metal centres adopt the pentagonal bipyramidal arrangement, while the metal centre in **1** adopts a trigonal bipyramidal arrangement. All the ligands containing the 4-(aminomethyl)pyridine moiety coordinated to the metal centre *via* the pyridyl nitrogen atom Ligands containing the 2-aminopyridine moiety coordinated to the metal centre *via* both the pyridyl nitrogen and the amide carbonyl. This tetradentate mode has previously been observed in similar ligand complexes.[8]

Fifteen of the sixteen coordination complexes formed 1-D polymeric chains, complexes **6** and **17** formed 2-D networks, while complex **7** is discrete and dinuclear**.** Except in complex **6,** the anions included in the crystal structure are not coordinated to the metal centre. They are located between 1-D chains and hydrogen bonding between these and water molecules (coordinated and uncoordinated) link the lower dimensional chains into higher dimensional networks.

Our studies have shown that by combining the rich coordination chemistry of pyridyl moiety and the hydrogen bonding ability of the amide groups, a range of coordination polymers can be constructed. Although the number of coordination complexes utilizing these ligands has increased significantly over the past decade, a variety of novel ligands can be constructed by varying the spacer unit as well as the donor atom position on the pyridyl moiety. The self assembly of these ligands with metal salts can result in coordination complexes with interesting properties.

5.2 References

1. L. J. Barbour, J. L. Atwood and G. O. Lloyd, *Chem. Commun.*, 2005, 1845.

2. G. W. Orr, J. L. Atwood and L. J. Barbour, *Nature*, 1998, **393**, 671.

3. R. Matsuda, S. Horike, S. Hasegawa, S. Furukawa, Y. Kinoshita, K. Mochizuki and S. Kitagawa, *J. Am. Chem. Soc.* 2007, **129**, 2607.

4. M. W. Hosseini, *CrystEngComm*, 2004, **6**, 318.

5. R. Taylor and O. Kennard, *Acc. Chem. Res*, 1984, **17**, 320.

6. N. N. Adarsh, D. K. Kumar, P. Dastidar, *Inorg. Chem. Commun,* 2008, **11**, 636.

7. Y. Wang, Y-Q. Hang, G-X. Liu, T-A. Okamura, M. Doi, Y-W. Sun and N. Ueyama, *Chem. Eur.J.*, 2007, **13**, 7523.

8. H-L. Hu, Y-F. Hsu, C-J. Wu, C-W. Yeh, D. M. Proserpio and J-D. Chen, *CrystEngComm,*, 2009, **11**, 168.

Appendices

The supplementary CD contains:

- **.**CIF files and .res files of the pure ligand;
- .CIF files and .res files of crystal structures **1-17;**
- NMR, MS, FTIR spectra of the pure ligands.